

Chemometric Optimization of $\text{BF}_3 \cdot \text{OEt}_2$ -Mediated Cyclization of Cannabidiol to Rare Δ^4 - and *iso*-THC Isomers

Arianna Bini,^[a] Lisa Rita Magnaghi,^[a] Valeria Cavalloro,^[b] Alessandra Bonanni,^[a] Stefano Protti,^{[a]*} Daniele Merli^{[a]*}

^[a] Department of Chemistry, University of Pavia, Viale Taramelli 10, 27100 Pavia, Italy

^[b] Department of Earth and Environmental Sciences, Via A. Ferrata 7, 27100 Pavia, Italy

Table Of Contents

1. Mass fragmentation of reported compounds	S2
2. Explorative reactions of CBD in the solvents considered	S10
3. Design of Experiments (DoE)	S26
4. ^1H and ^{13}C NMR Spectra for the isolated compounds	S30

1. Mass fragmentation of reported compounds

1.1. CBD

The ten major peaks in the mass fragmentation spectra of this compound are:

<i>m/z</i>	231	68	67	55	174	53	232	91	175	77
<i>Relative abundance</i>	999	541	523	217	199	162	149	120	89	83

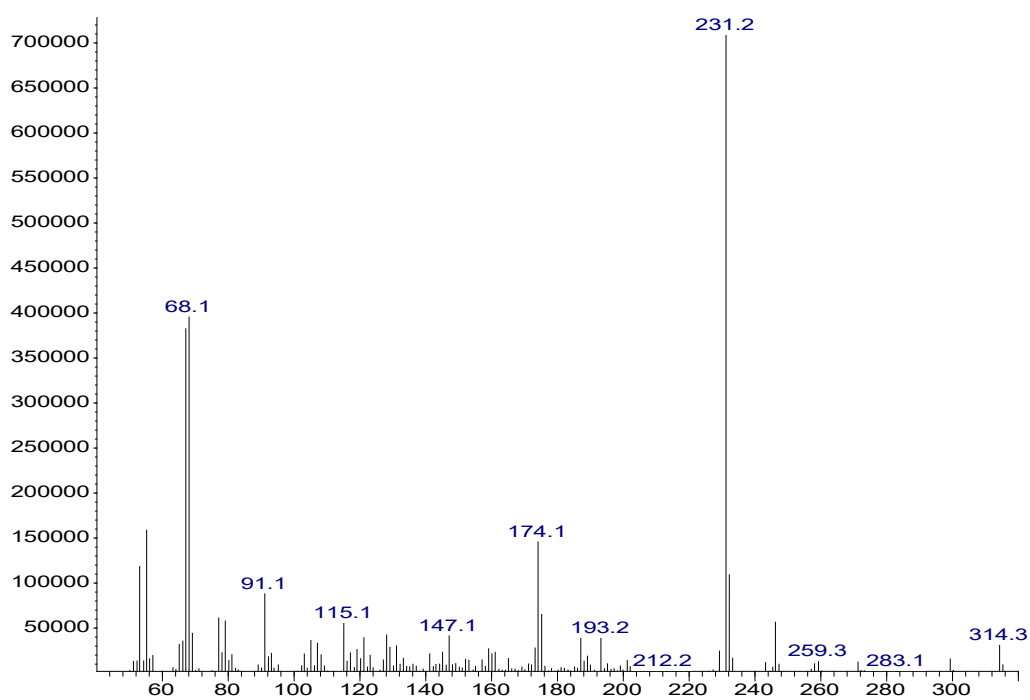


Fig. S1 Mass fragmentation of CBD.

1.2. Δ^4 -iso-THC

The ten major peaks in the mass fragmentation spectra of this compound are:

<i>m/z</i>	271	314	55	231	67	201	91	272	193	174
<i>Relative abundance</i>	999	381	304	303	242	242	197	194	171	163

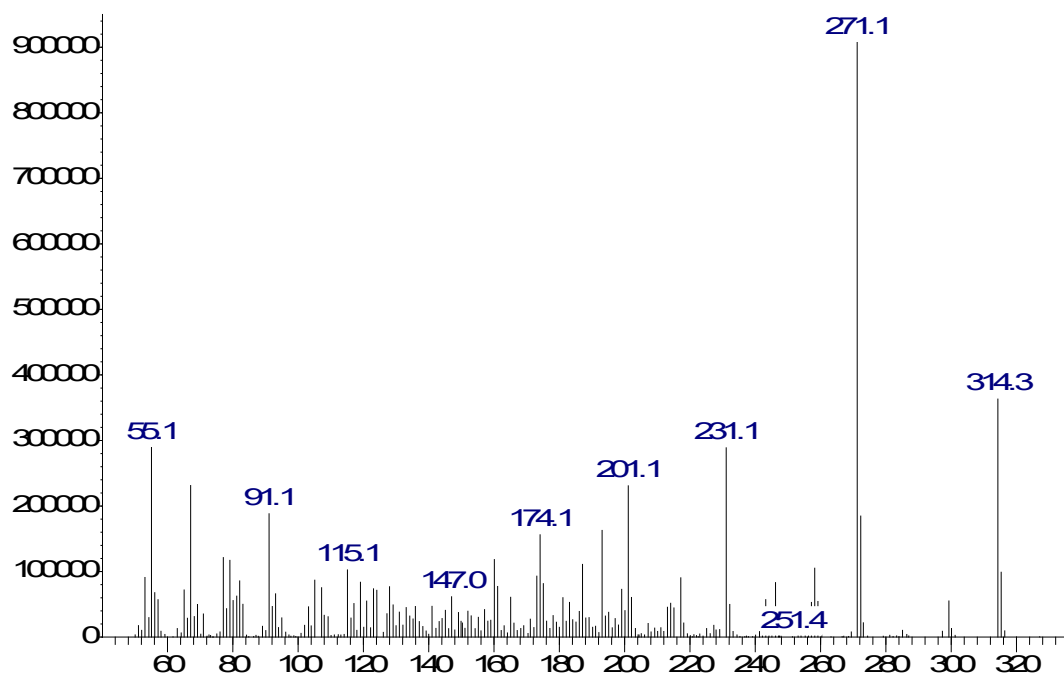


Fig. S2 Mass fragmentation of Δ^4 -iso-THC.

1.3. $\Delta^4(8)$ -iso-THC

The ten major peaks in the mass fragmentation spectra of this compound are:

<i>m/z</i>	271	314	231	55	258	299	91	67	187	174
<i>Relative abundance</i>	999	845	820	702	451	408	395	369	311	304

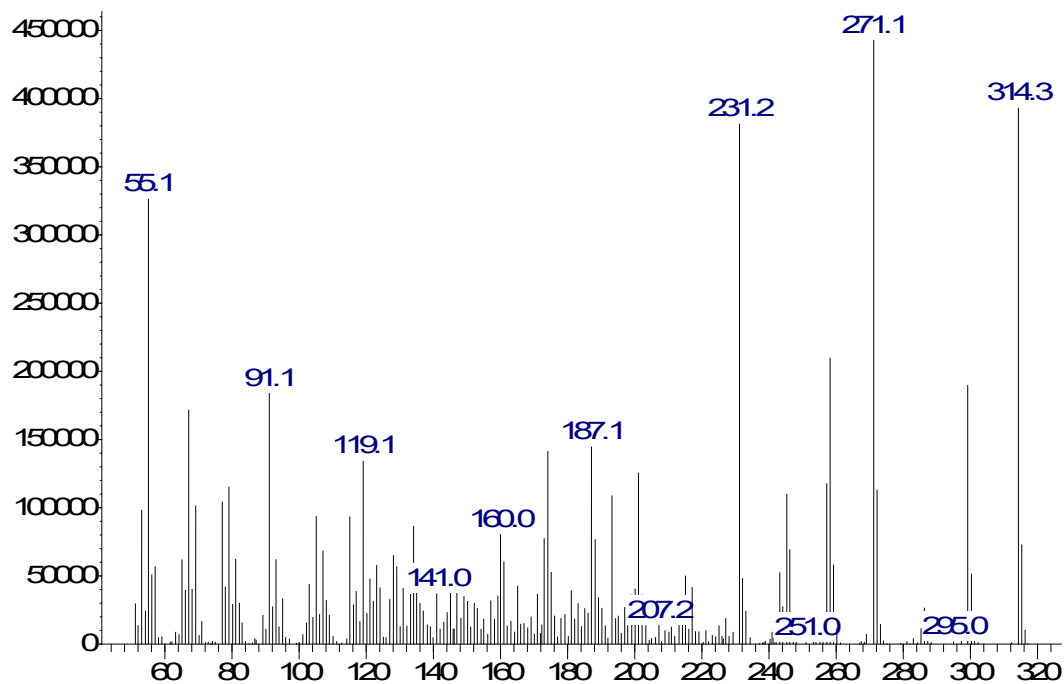


Fig. S3 Mass fragmentation of $\Delta^4(8)$ -iso-THC.

1.4. Δ^8 -iso-THC

The ten major peaks in the mass fragmentation spectra of this compound are:

<i>m/z</i>	231	67	55	174	232	314	68	81	233	91
<i>Relative abundance</i>	999	216	195	165	152	118	110	95	84	79

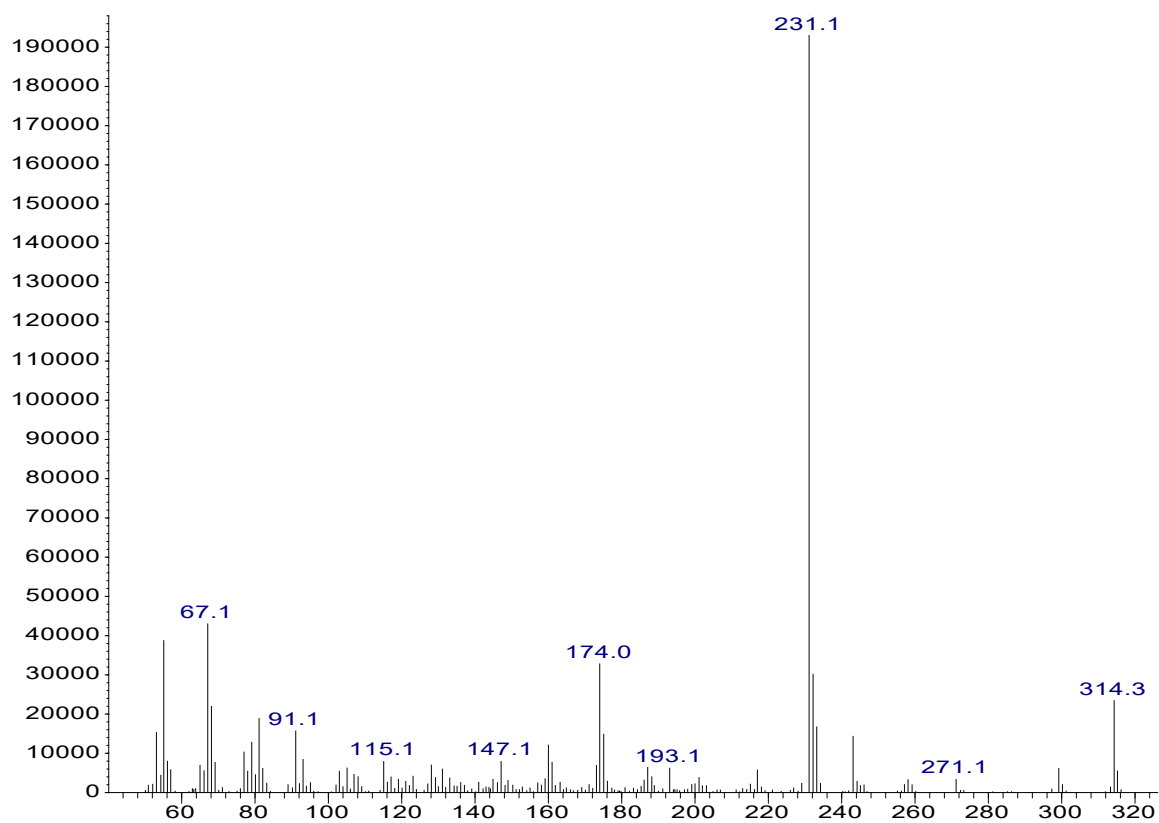


Fig. S4 Mass fragmentation of Δ^8 -iso-THC.

1.5. *t*Bu- Δ^9 -THC

The ten major peaks in the mass fragmentation spectra of this compound are:

<i>m/z</i>	57	299	314	231	271	243	258	315	300	55
<i>Relative abundance</i>	999	397	382	199	160	104	103	89	77	76

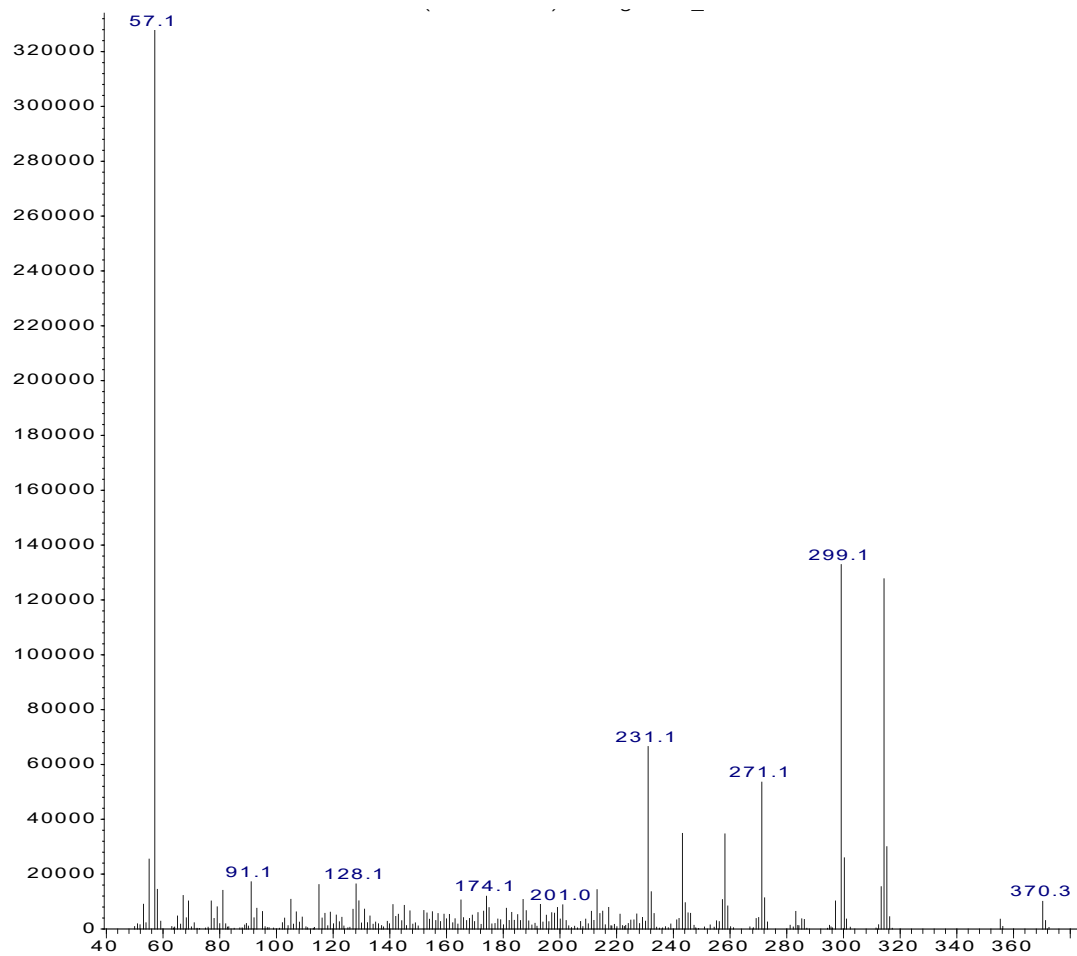


Fig. S5 Mass fragmentation of *t*Bu- Δ^9 -THC.

1.6. MeCN- $\Delta^{4(8)}$ -iso-THC

The ten major peaks in the mass fragmentation spectra of this compound are:

<i>m/z</i>	231	314	271	232	174	55	258	299	69	91
<i>Relative abundance</i>	999	362	333	216	193	192	178	173	159	156

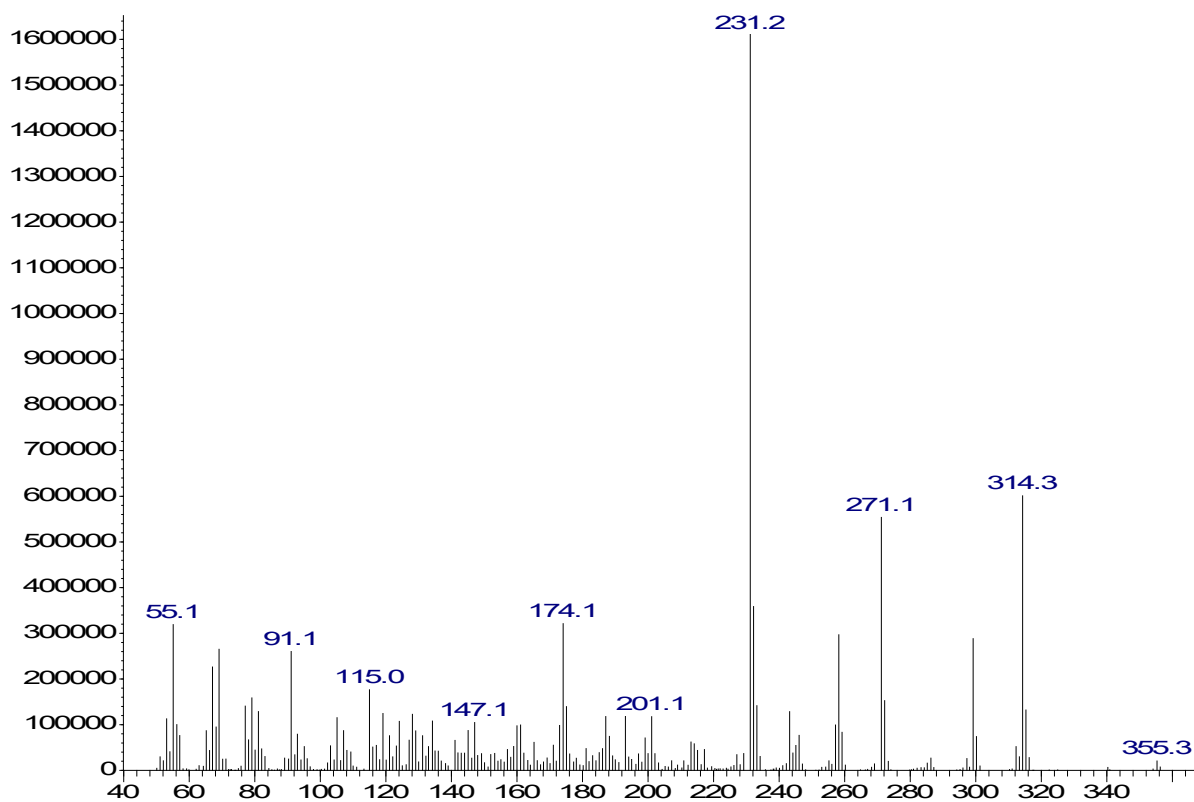


Fig. S6 Mass fragmentation of MeCN- $\Delta^{4(8)}$ -iso-THC.

1.7. Δ^8 -THC

The ten major peaks in the mass fragmentation spectra of this compound are:

<i>m/z</i>	231	314	67	258	68	55	271	174	91	53
<i>Relative abundance</i>	999	437	384	274	259	246	227	226	216	161

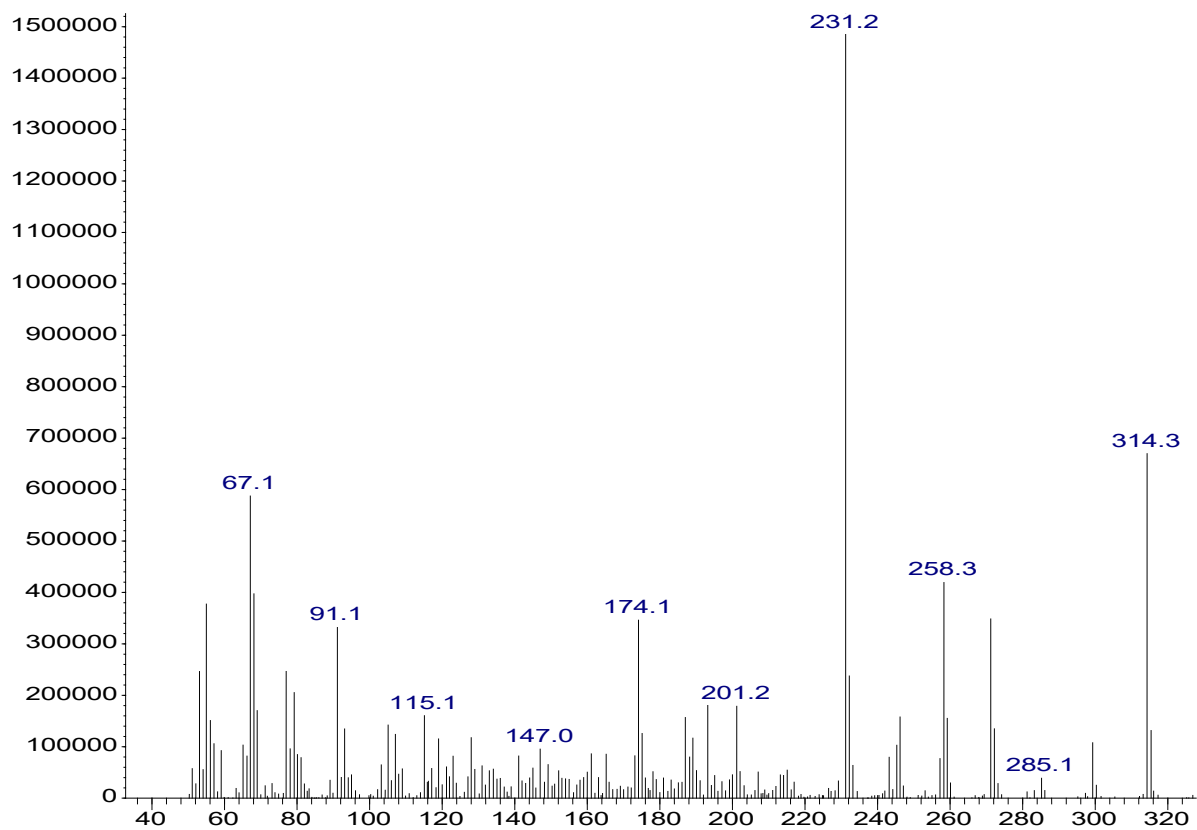


Fig. S7 Mass fragmentation of MeCN- Δ^8 -iso-THC.

1.8. Δ^9 -THC

The ten major peaks in the mass fragmentation spectra of this compound are:

<i>m/z</i>	299	314	231	271	55	91	243	67	77	300
<i>Relative abundance</i>	999	826	684	467	415	339	338	250	233	223

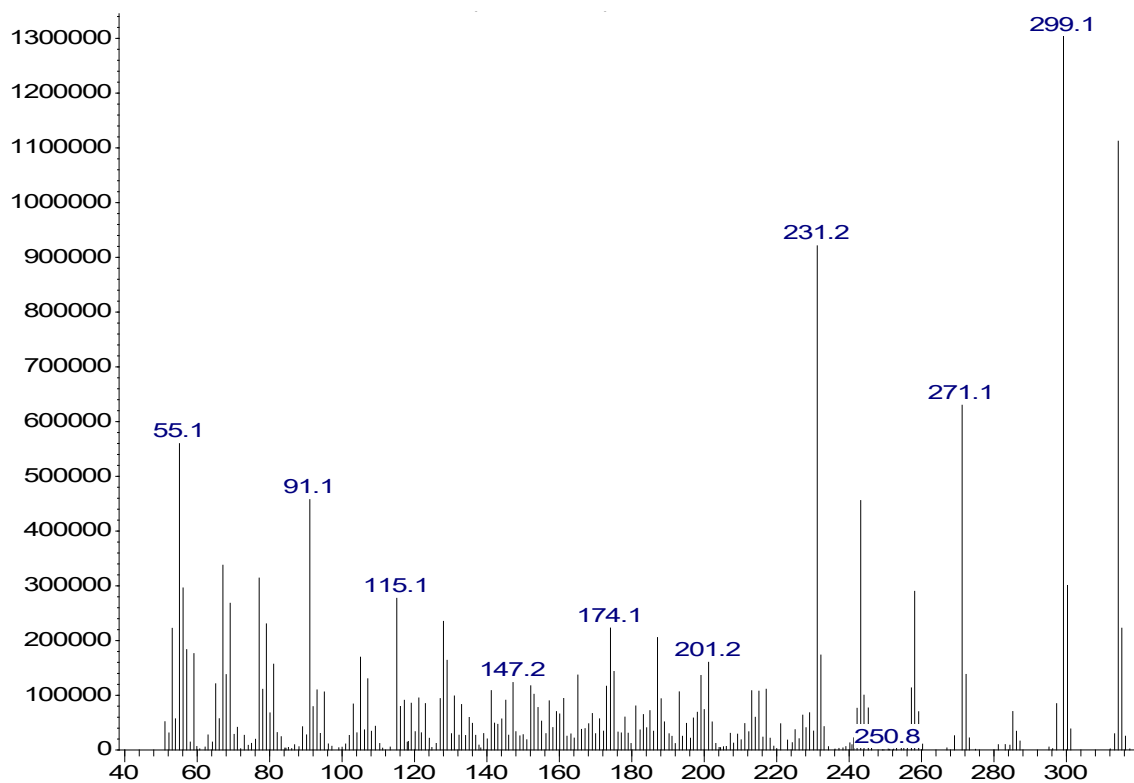


Fig. S8 Mass fragmentation of Δ^9 -THC.

2. Explorative reactions of CBD in the solvents considered

2.1. Toluene

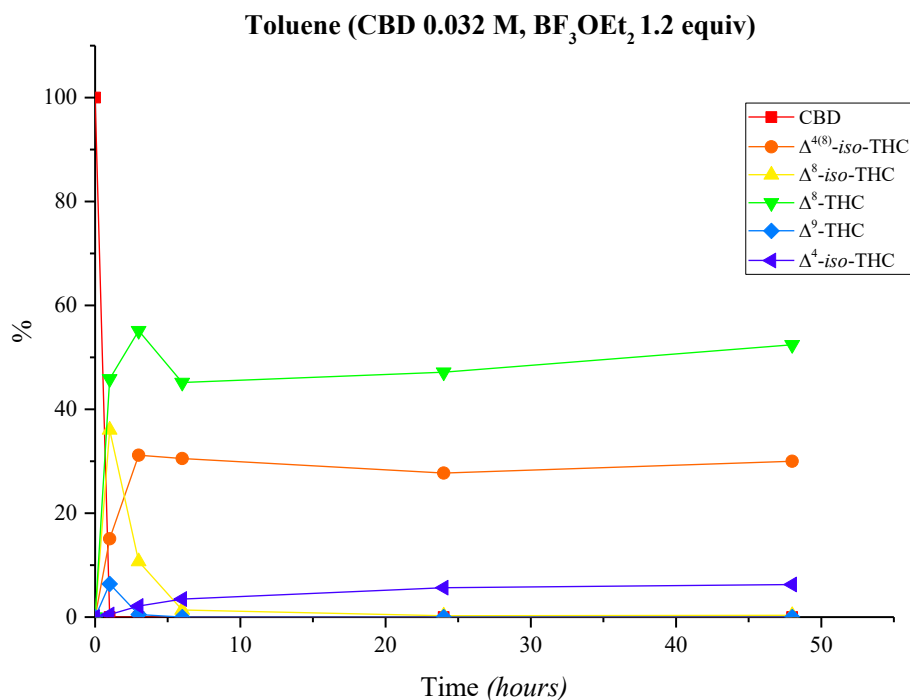


Fig. S9 Time-dependent consumption of CBD and product formation. Conditions: CBD 0.032 M, BF₃OEt₂ 1.2 equivalents.

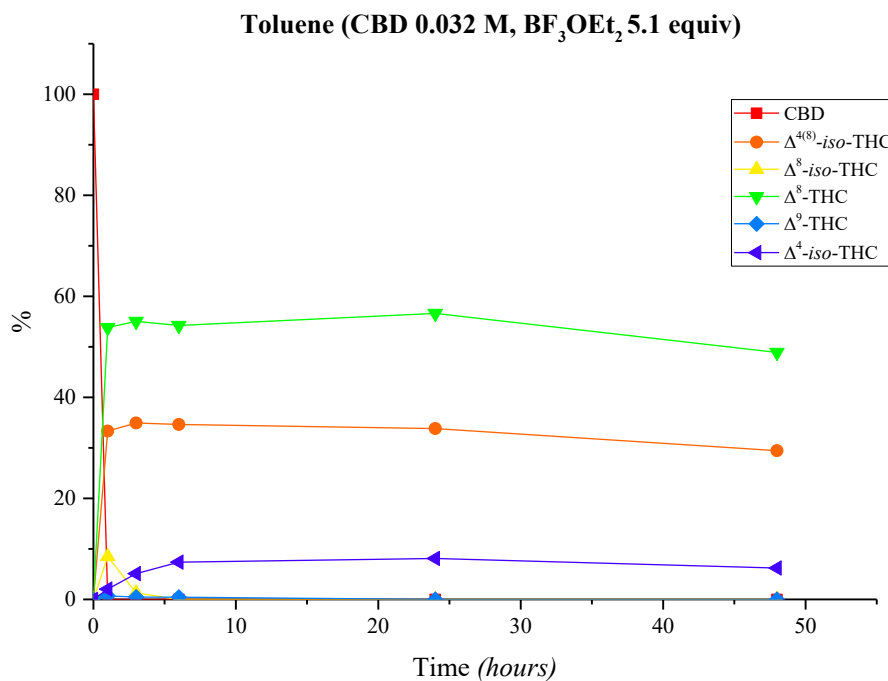


Fig. S10 Time-dependent consumption of CBD and product formation in toluene. Conditions: CBD 0.032 M, BF₃OEt₂ 5.1 equivalents.

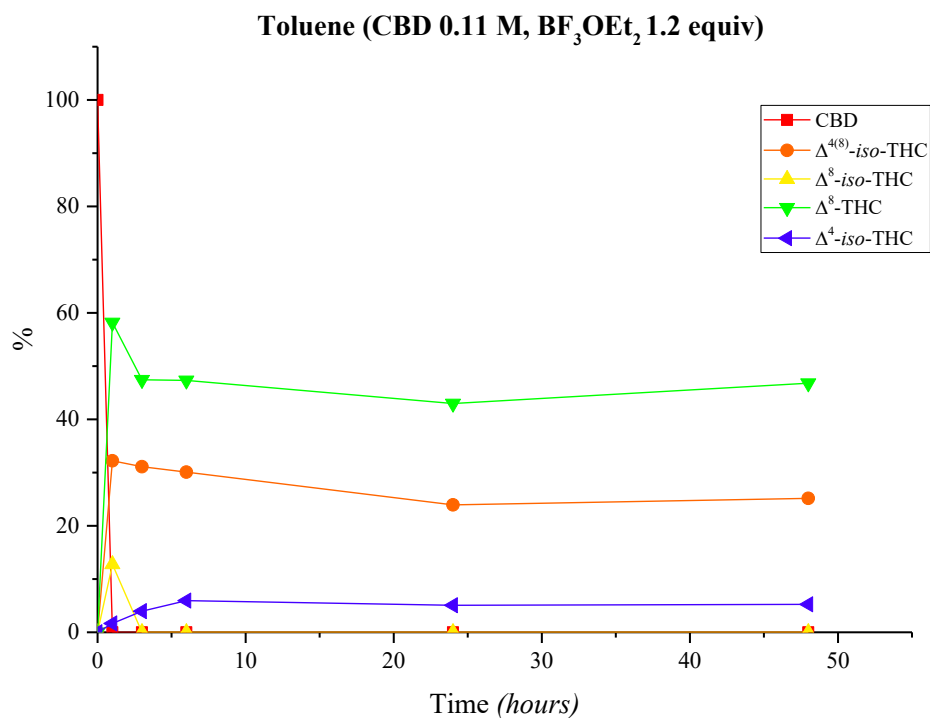


Fig. S11 Time-dependent consumption of CBD and product formation in toluene. Conditions: CBD 0.11 M, BF₃OEt₂ 1.2 equivalents.

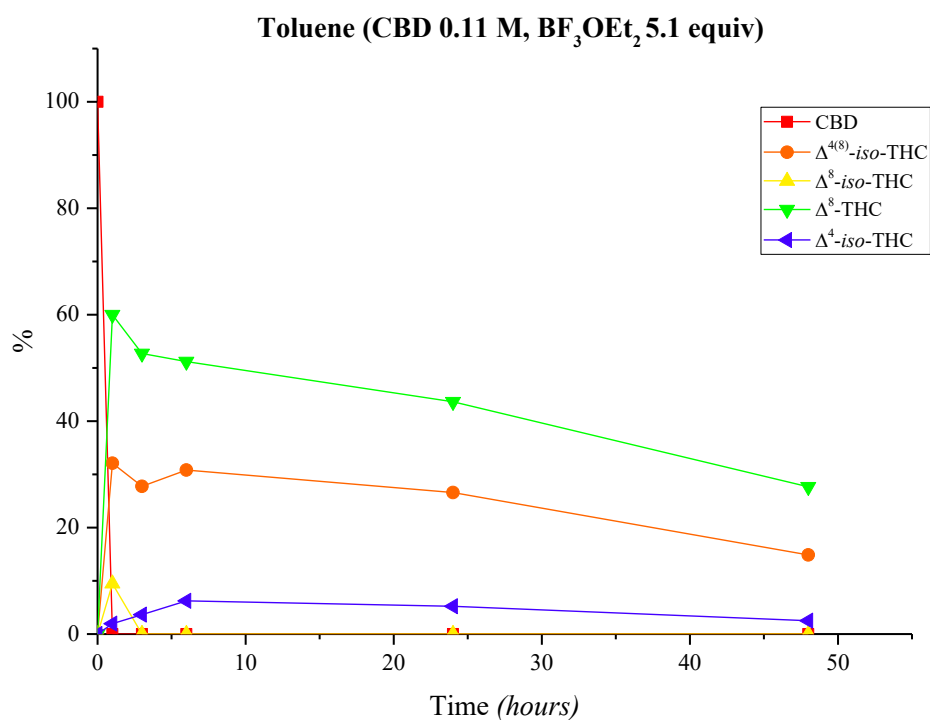


Fig. S12 Time-dependent consumption of CBD and product formation in toluene. Conditions: CBD 0.11 M, BF₃OEt₂ 5.1 equivalents.

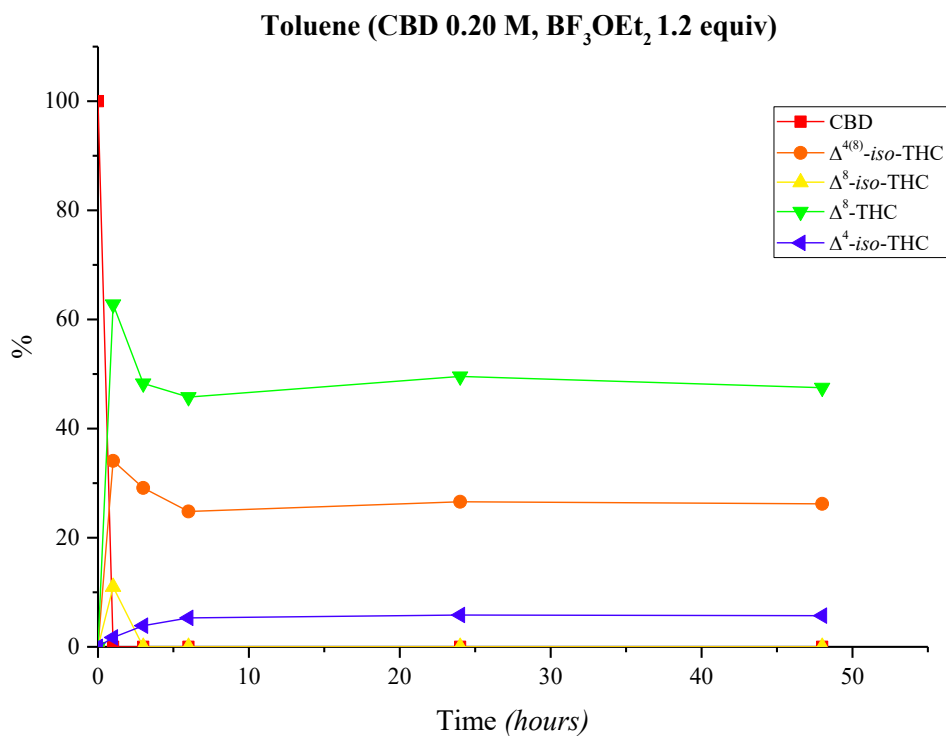


Fig. S13 Time-dependent consumption of CBD and product formation in toluene. Conditions: CBD 0.20 M, BF₃OEt₂ 1.2 equivalents.

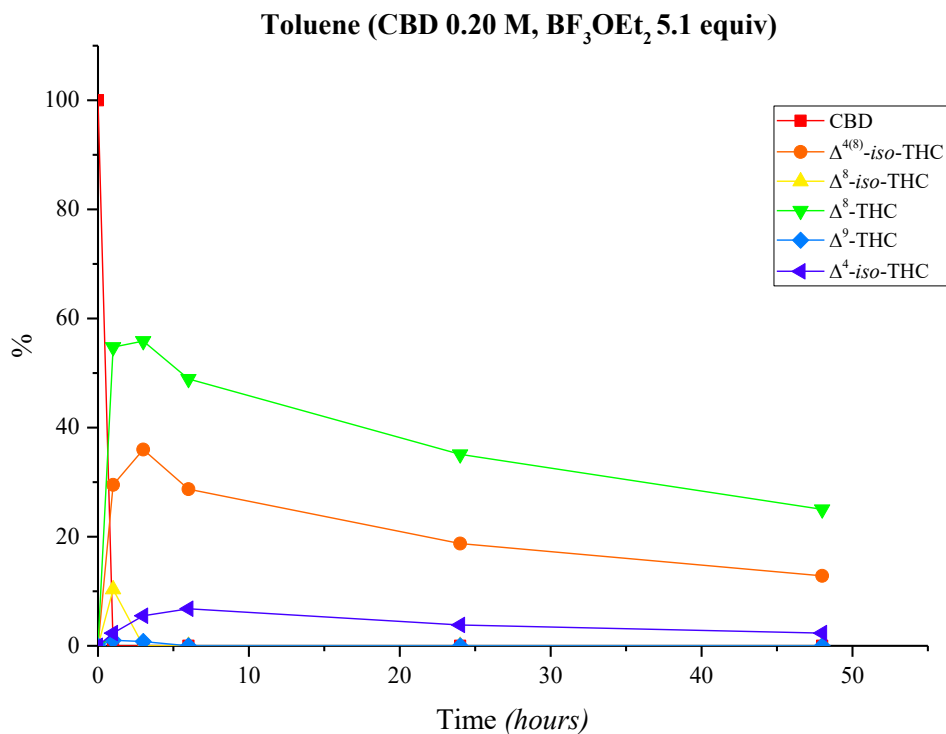


Fig. S14 Time-dependent consumption of CBD and product formation in toluene. Conditions: CBD 0.20 M, BF₃OEt₂ 5.1 equivalents.

As apparent from Figures S9-S14, CBD in Toluene is efficiently converted to Δ^8 -THC (main product, that has been detected in up to 63% yield, when a 0.20 M solution of CBD has been treated with 1.2 equiv. of BF_3OEt_2 , see Figure S13) and $\Delta^{4(8)}$ -*iso*-THC. Δ^4 -*iso*-THC was also observed as secondary product, derived from the acid catalyzed isomerization of $\Delta^{4(8)}$ -*iso*-THC.

2.2. α, α, α -trifluorotoluene

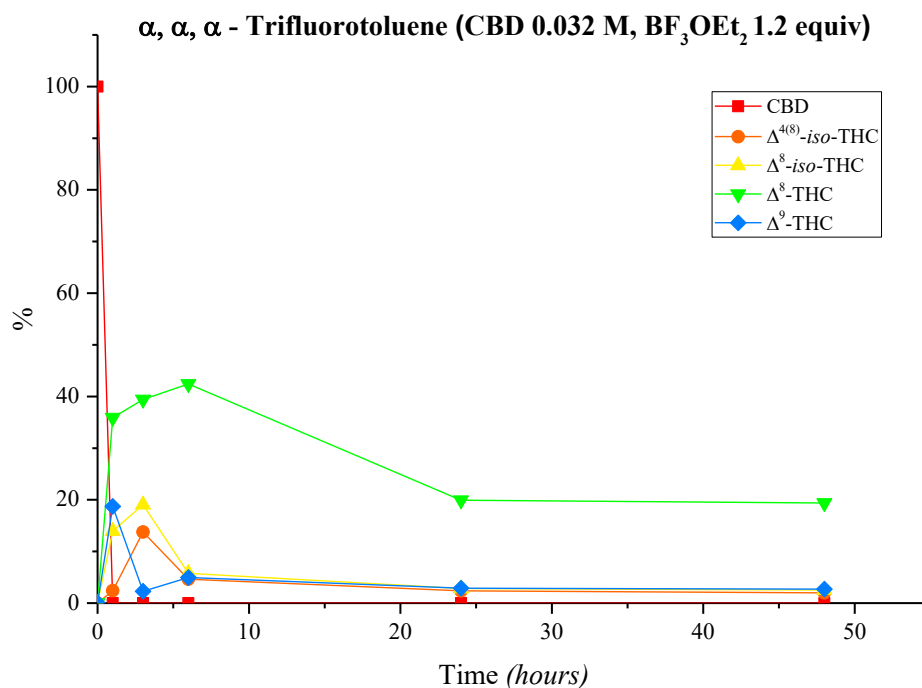


Fig. S15 Time-dependent consumption of CBD and product formation in α, α, α - trifluorotoluene. Conditions: CBD 0.032 M, BF_3OEt_2 1.2 equivalents.

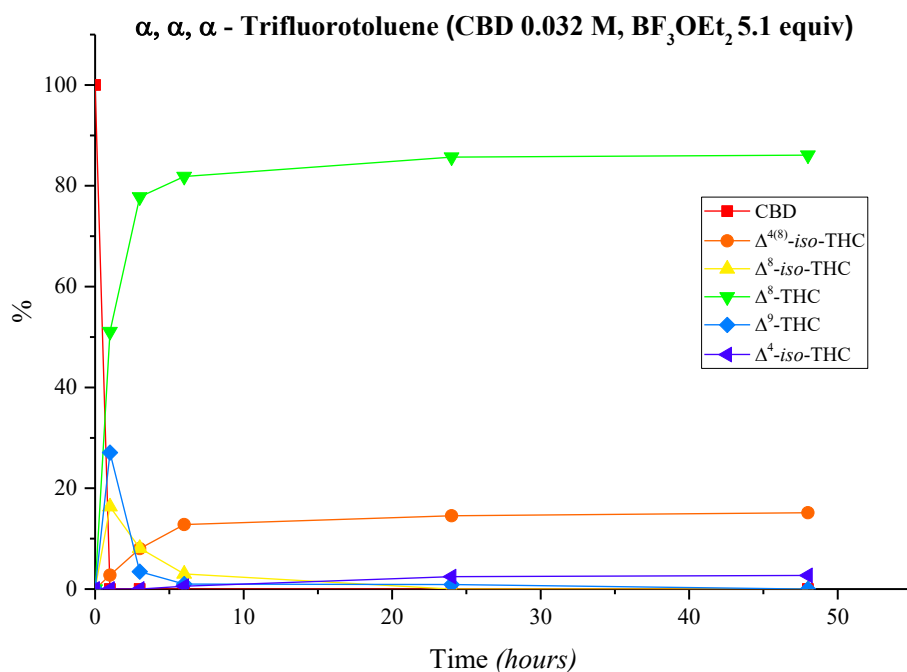


Fig. S16 Time-dependent consumption of CBD and product formation in α, α, α - trifluorotoluene. Conditions: CBD 0.032 M, BF_3OEt_2 5.1 equivalents.

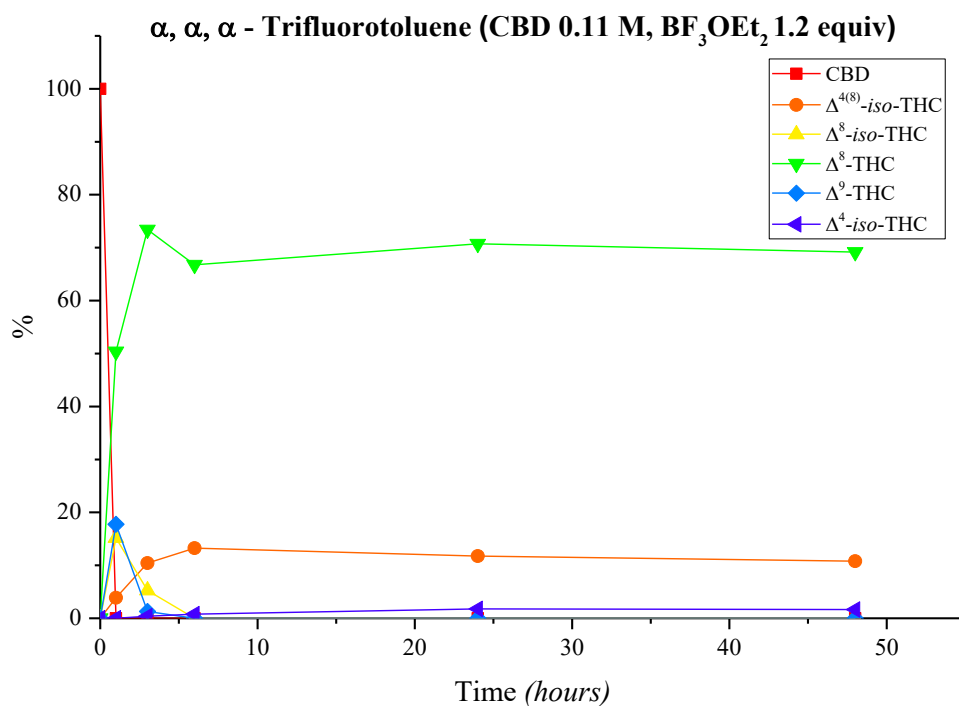


Fig. S17 Time-dependent consumption of CBD and product formation in α, α, α - trifluorotoluene. Conditions: CBD 0.11 M, BF_3OEt_2 1.2 equivalents.

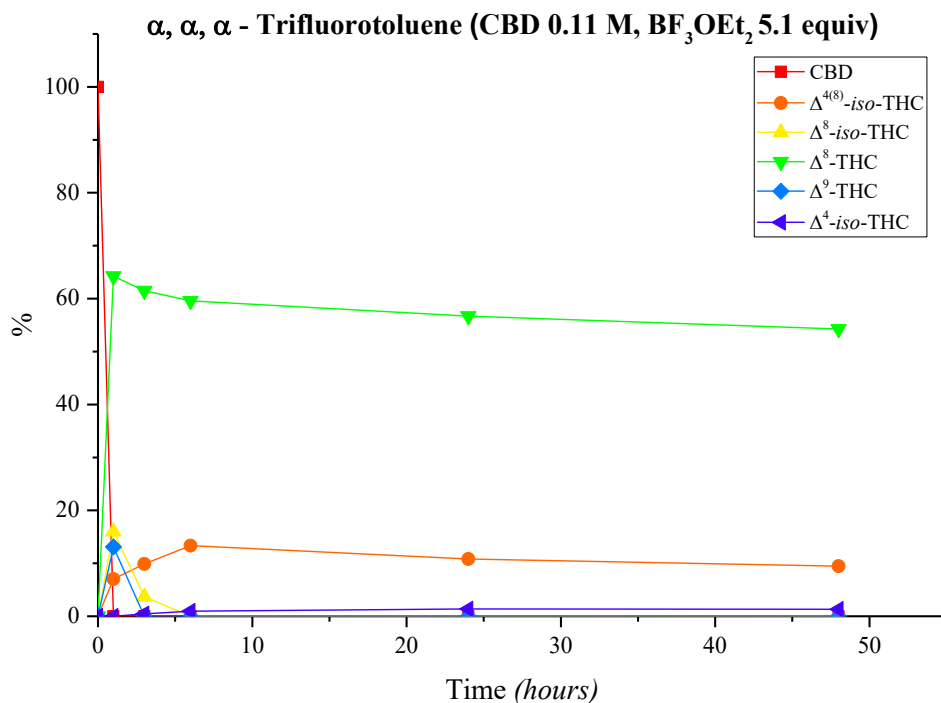


Fig. S18 Time-dependent consumption of CBD and product formation in α, α, α - trifluorotoluene. Conditions: CBD 0.11 M, BF_3OEt_2 5.1 equivalents.

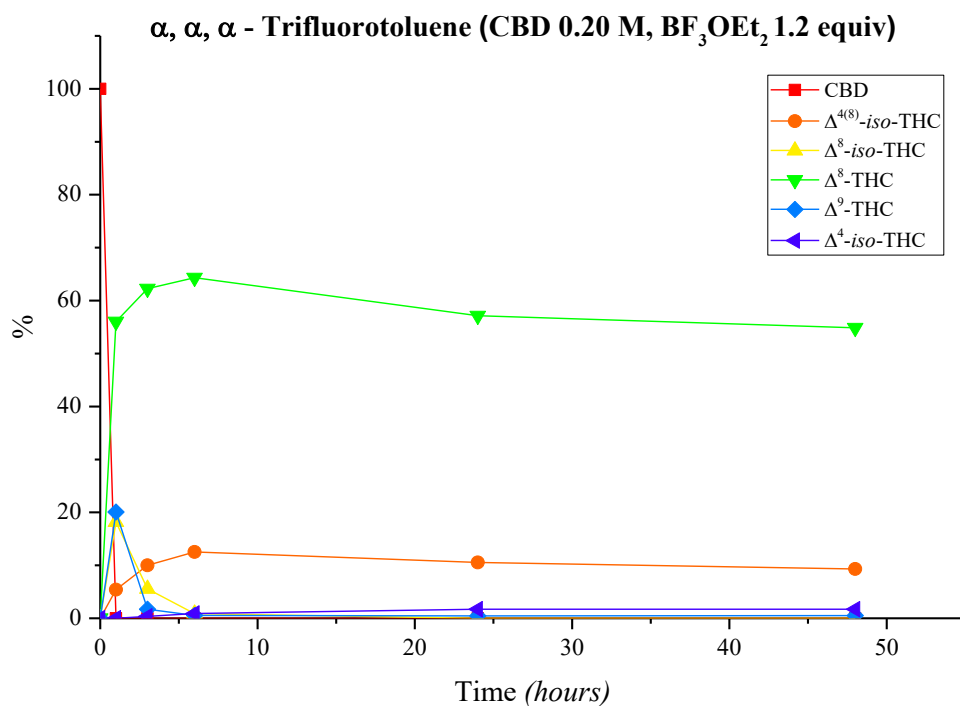


Fig. S19 Time-dependent consumption of CBD and product formation in α, α, α - trifluorotoluene. Conditions: CBD 0.20 M, BF_3OEt_2 1.2 equivalents.

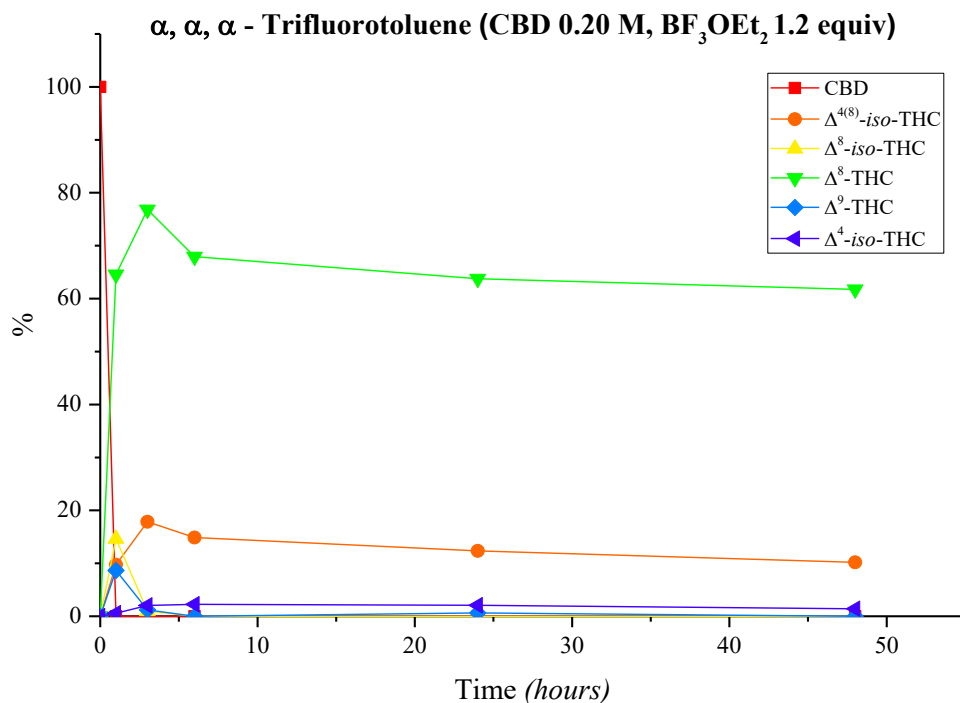


Fig. S20 Time-dependent consumption of CBD and product formation in α, α, α - trifluorotoluene. Conditions: CBD 0.20 M, BF_3OEt_2 5.1 equivalents.

As depicted in Figures S15-S20, Δ^8 -THC is the main product obtained from the treatment of CBD with BF_3OEt_2 in α,α,α -Trifluorotoluene, along with a minor amount of $\Delta^{4(8)}$ -*iso*-THC. Low concentrations of Δ^9 -THC were observed at short reaction times (< 5 h). The conversion process achieves an almost quantitative efficiency under the conditions described in Fig. S16 (a 0.032 M solution of CBD treated with 5.1 equiv. of BF_3OEt_2).

2.3. MTBE

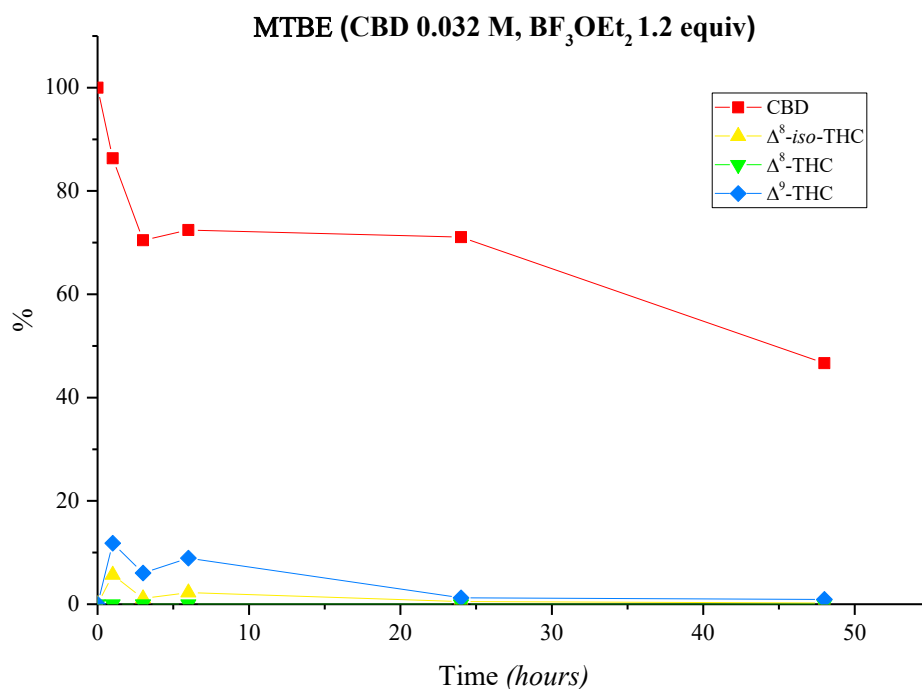


Fig. S21 Time-dependent consumption of CBD and product formation in MTBE. Conditions: CBD 0.032 M, BF₃OEt₂ 1.2 equivalents.

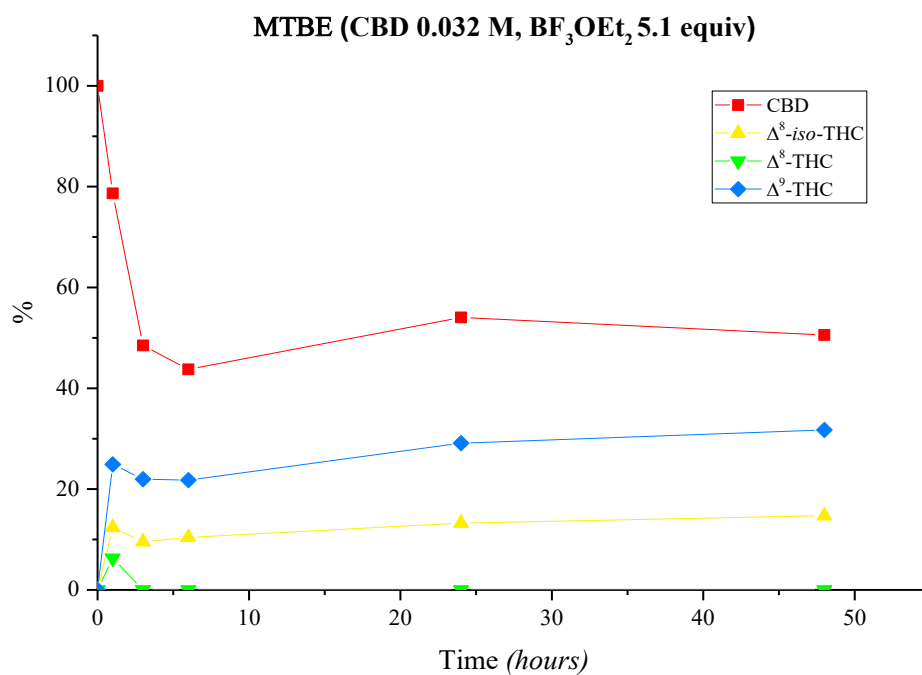


Fig. S22 Time-dependent consumption of CBD and product formation in MTBE. Conditions: CBD 0.032 M, BF₃OEt₂ 5.1 equivalents.

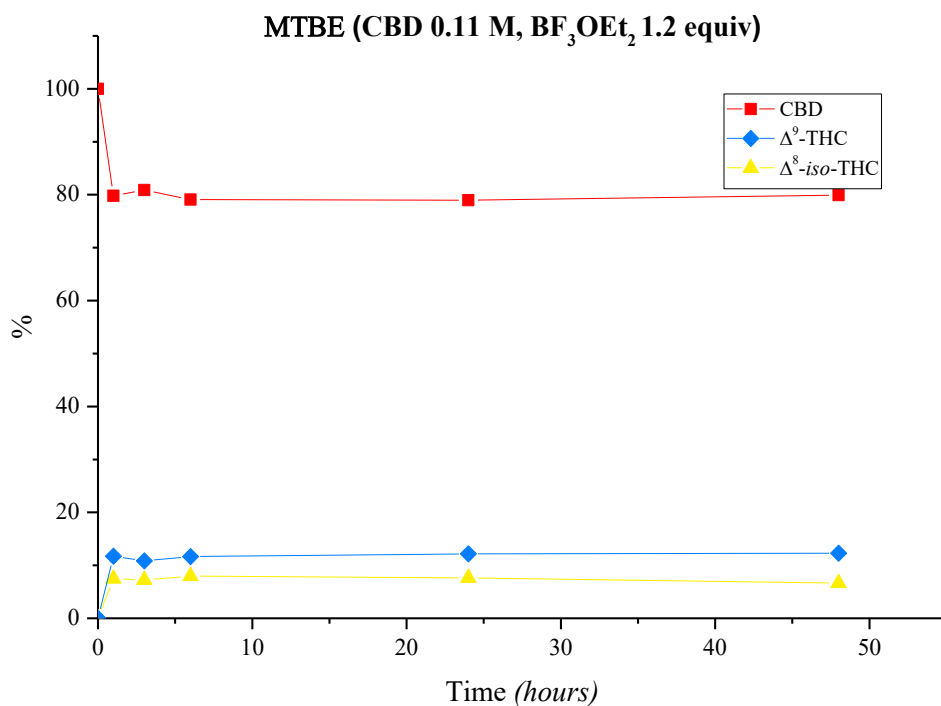


Fig. S23 Time-dependent consumption of CBD and product formation in MTBE. Conditions: CBD 0.11 M, BF₃OEt₂ 1.2 equivalents.

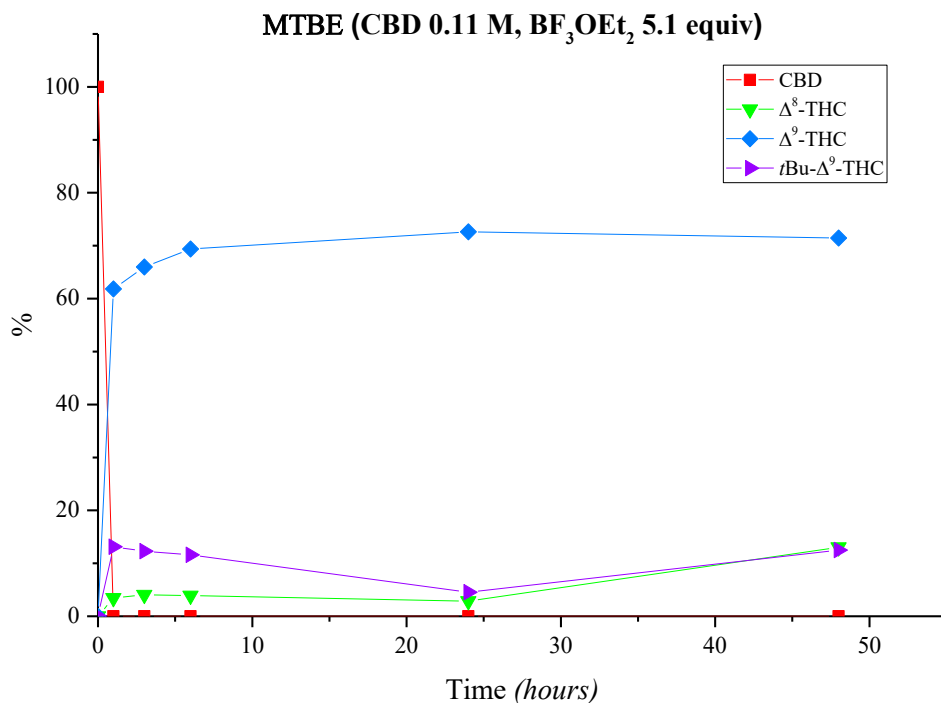


Fig. S24 Time-dependent consumption of CBD and product formation in MTBE. Conditions: CBD 0.11 M, BF₃OEt₂ 5.1 equivalents.

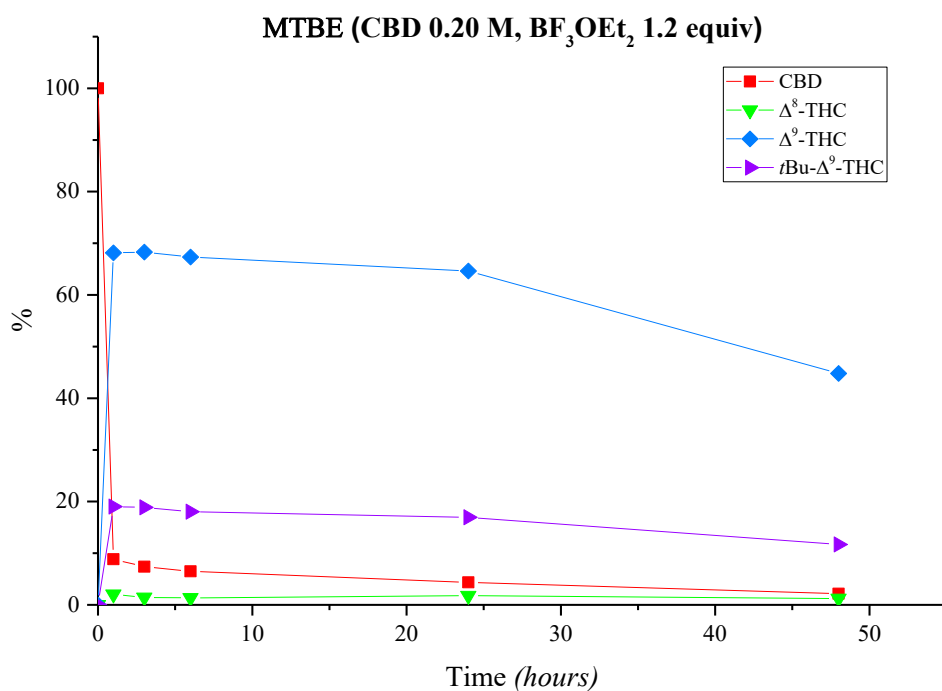


Fig. S25 Time-dependent consumption of CBD and product formation in MTBE. Conditions: CBD 0.20 M, BF₃OEt₂ 1.2 equivalents.

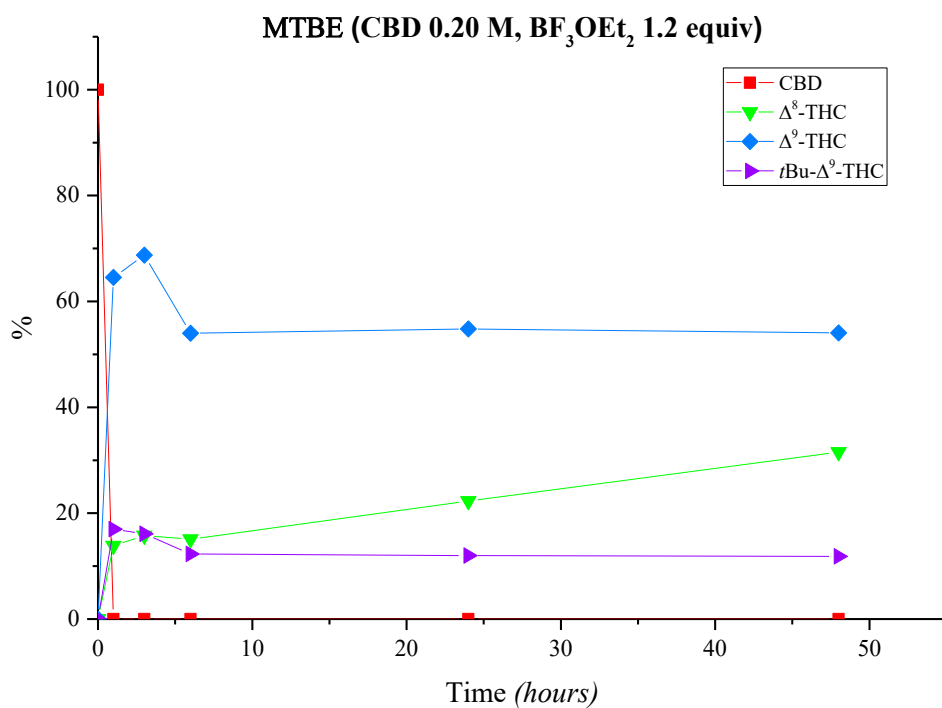


Fig. S26 Time-dependent consumption of CBD and product formation in MTBE. Conditions: CBD 0.20 M, BF₃OEt₂ 5.1 equivalents.

As depicted in Figures S21-S26, Δ^9 -THC is the main product obtained from the treatment of CBD at high concentration with BF_3OEt_2 along with minor amounts of tBu- Δ^9 -THC. When the same process was carried out on diluted solutions of CBD, no significant conversion of the starting substrate was observed.

2.4. MeCN

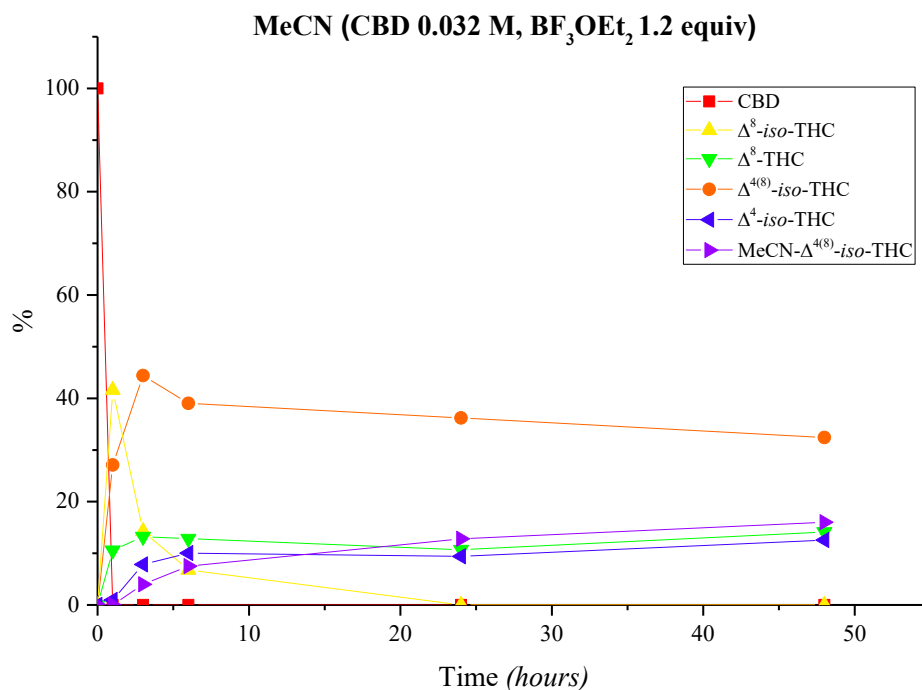


Fig. S27 Time-dependent consumption of CBD and product formation in acetonitrile. Conditions: CBD 0.032 M, BF₃OEt₂ 1.2 equivalents.

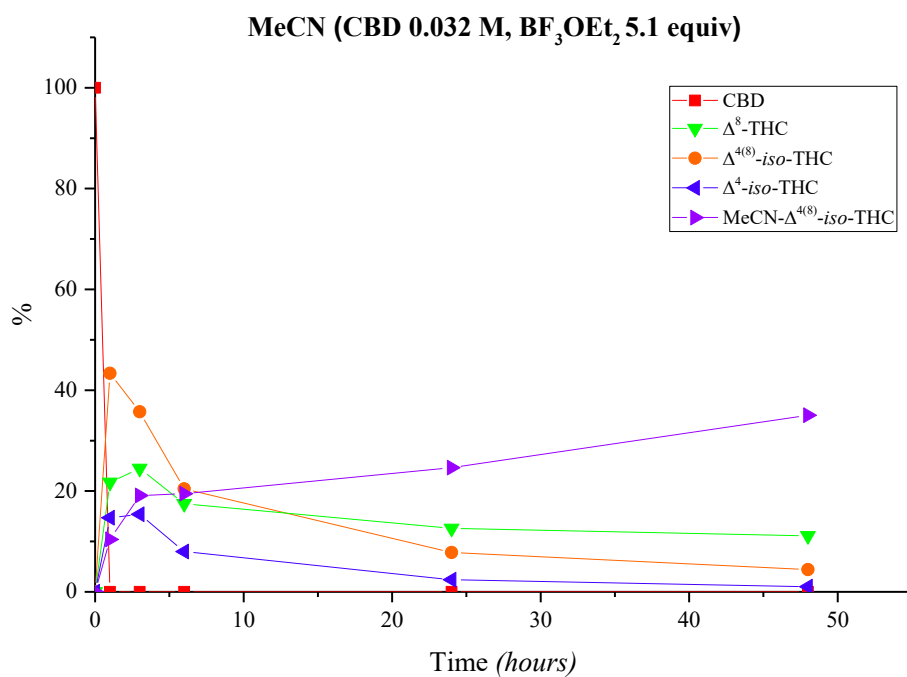


Fig. S28 Time-dependent consumption of CBD and product formation in acetonitrile. Conditions: CBD 0.032 M, BF₃OEt₂ 5.1 equivalents.

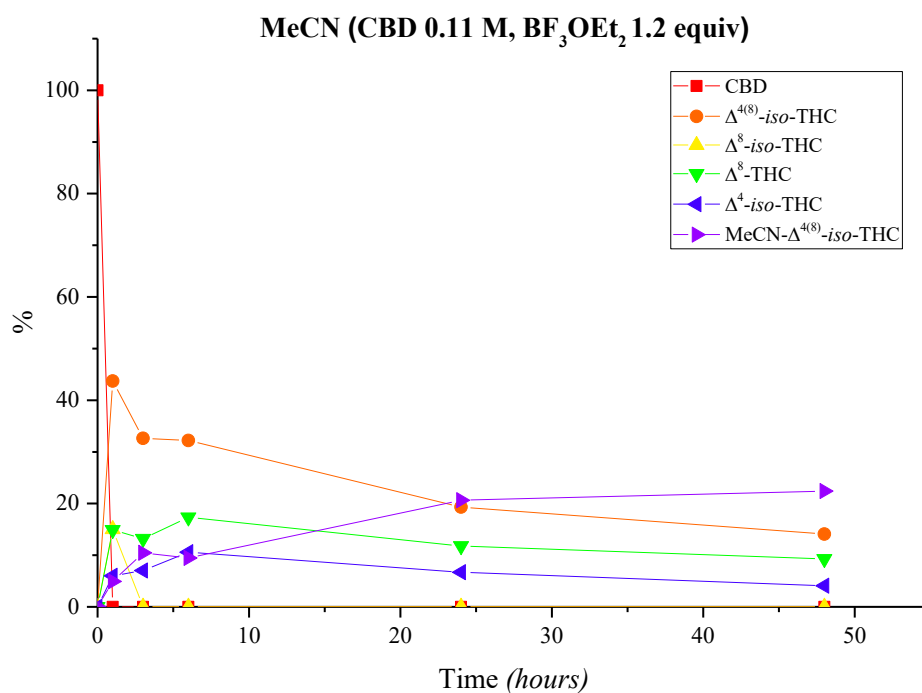


Fig. S29 Time-dependent consumption of CBD and product formation in acetonitrile. Conditions: CBD 0.11 M, BF₃OEt₂ 1.2 equivalents.

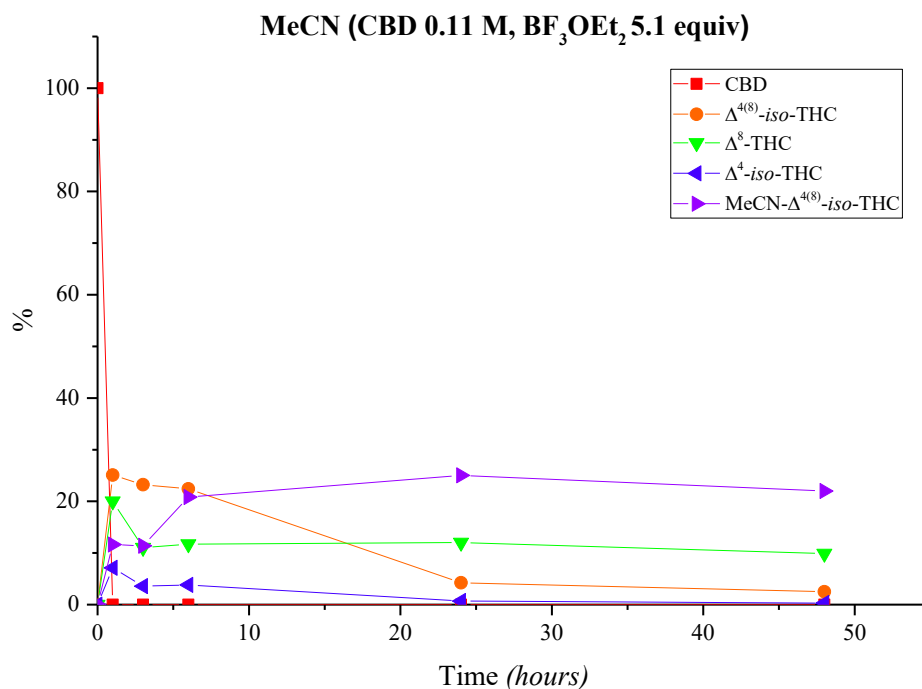


Fig. S30 Time-dependent consumption of CBD and product formation in acetonitrile. Conditions: CBD 0.11 M, BF₃OEt₂ 5.1 equivalents.

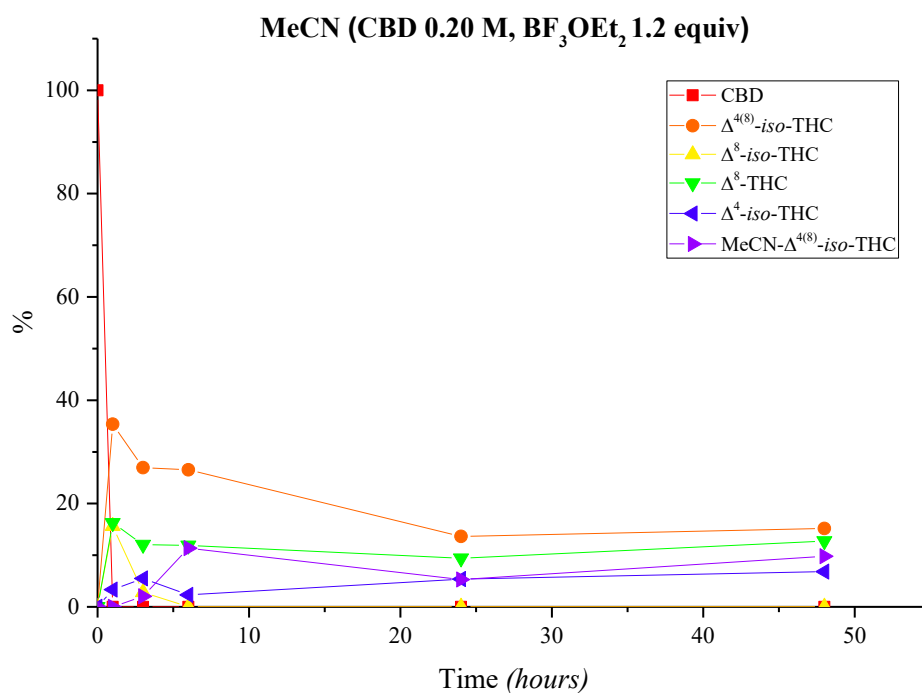


Fig. S31 Time-dependent consumption of CBD and product formation in acetonitrile. Conditions: CBD 0.20 M, BF₃OEt₂ 1.2 equivalents.

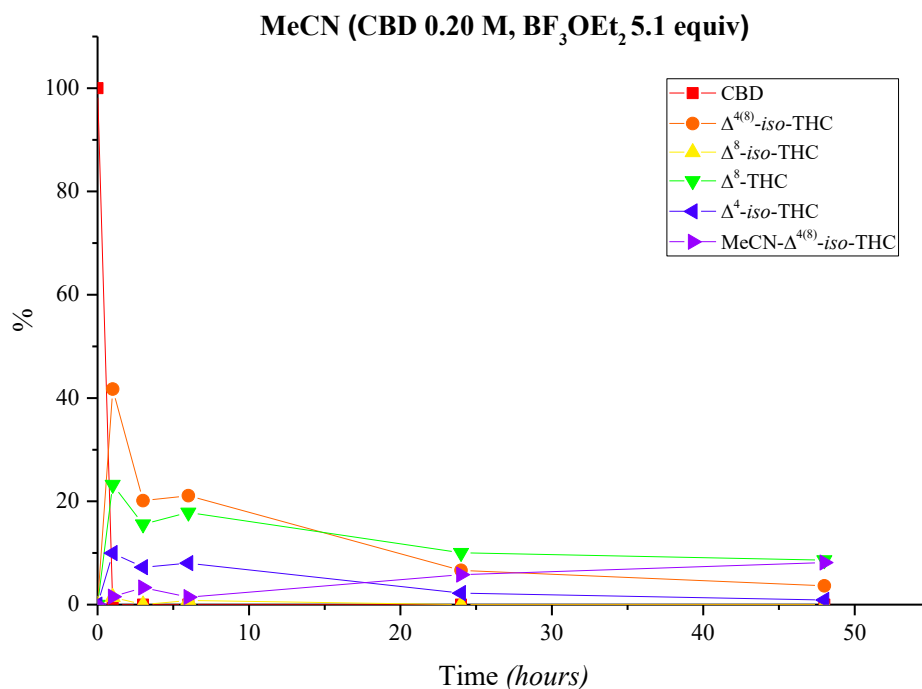


Fig. S32 Time-dependent consumption of CBD and product formation in acetonitrile. Conditions: CBD 0.20 M, BF₃OEt₂ 5.1 equivalents.

As depicted in Figures S27-S32, in MeCN the formation $\Delta^{4(8)}$ -iso-THC is followed by its partial conversion to the corresponding MeCN- $\Delta^{4(8)}$ -iso-THC, that has been observed in high yield under the reaction conditions adopted in figure S28 (a 0.032 M solution of CBD treated with 5.1 equiv of BF_3OEt_2). In most cases, low amounts of Δ^8 -THC and Δ^4 -*iso*-THC have been also detected.

3. Design of Experiments (DoE)

3.1. 2³ full factorial Design of Experiments

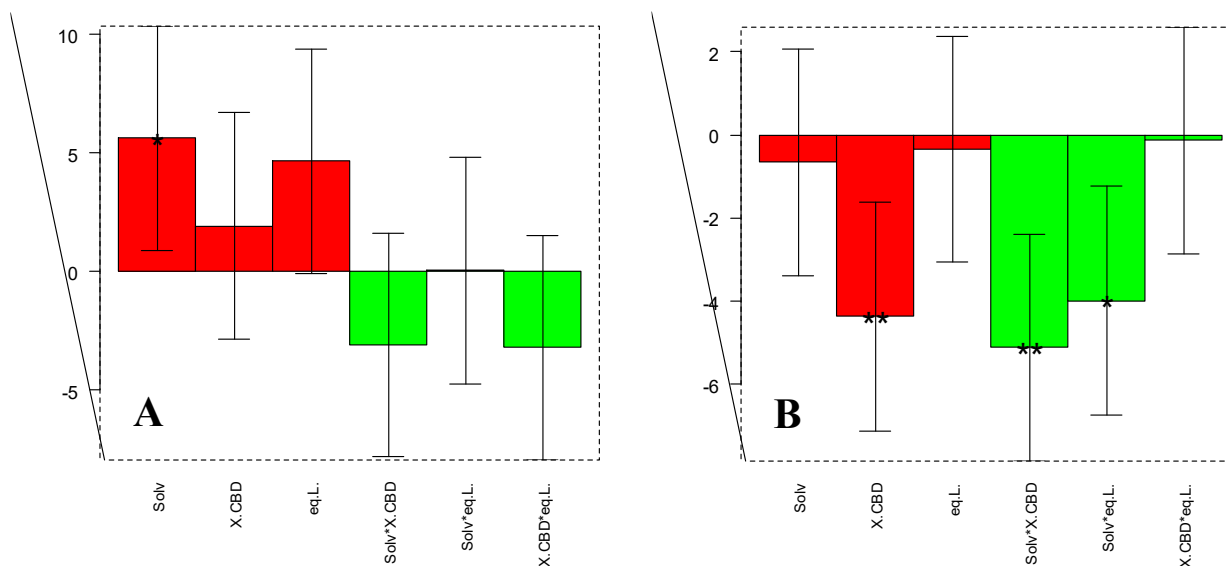


Fig. S33 Coefficient plots relative to the FFD on $\Delta^{4(8)}$ -iso-THC, respectively to [A] 1 hour of reaction time and [B] 3 hours of reaction time. The asterisks, when present, indicate a significant influence of the respective parameters or their interaction and significance (* $p \leq 0.05$, ** $p \leq 0.01$, *** $p \leq 0.001$).

FFD on $\Delta^{4(8)}$ -iso-THC yield				
Coefficient	1 hour		3 hours	
	Value	Significance	Value	Significance
b_0	32.4		31.1	
b_1	5.6	*	-0.7	
b_2	1.9		-4.4	**
b_3	4.7		-0.3	
b_{12}	-3.1		-5.1	**
b_{13}	0.0		-4.0	*
b_{23}	-3.2		-0.1	

Table S1 Coefficient values and their significance (* $p \leq 0.05$, ** $p \leq 0.01$, *** $p \leq 0.001$ relative to the FFD on $\Delta^{4(8)}$ -iso-THC.

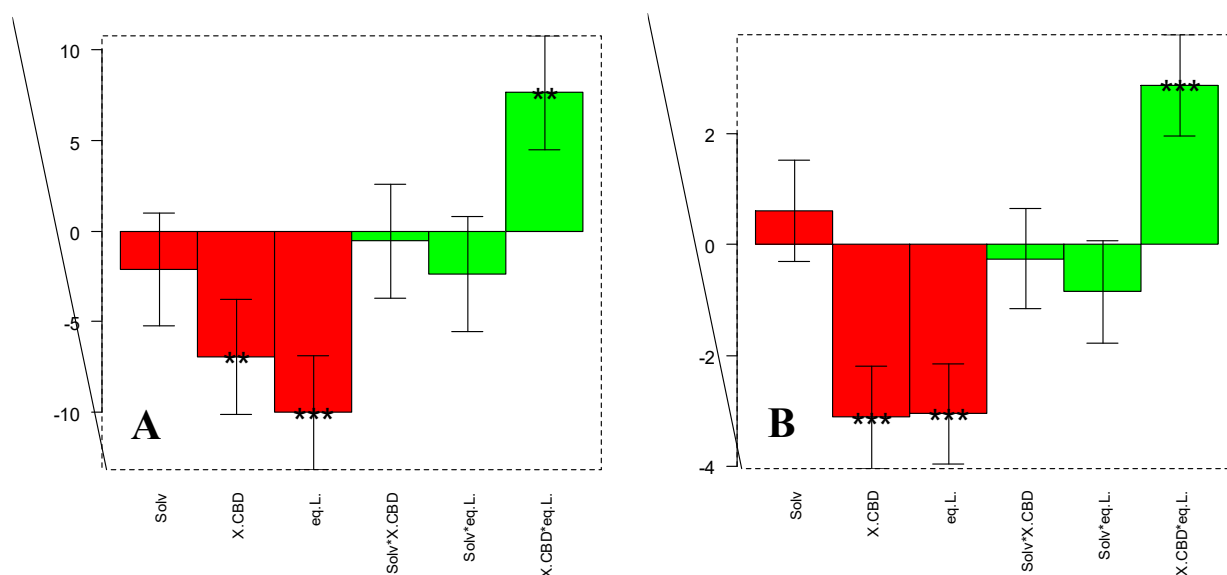


Fig. S34 Coefficient plots relative to the FFD on Δ^8 -iso-THC, respectively to [A] 1 hour of reaction time and [B] 3 hours of reaction time. The asterisks, when present, indicate a significant influence of the respective parameters or their interaction and significance (* $p \leq 0.05$, ** $p \leq 0.01$, *** $p \leq 0.001$).

FFD for the optimization of Δ^8 -iso-THC yield				
Coefficient	1 hour		3 hours	
	Value	Significance	Value	Significance
b_0	14.9		3.5	
b_1	-2.1		0.6	
b_2	-6.9	**	-3.1	***
b_3	-10.0	***	-3.1	***
b_{12}	-0.6		-0.3	
b_{13}	-2.4		-0.9	
b_{23}	7.6	**	2.9	***

Table S2 Coefficient values and their significance (* $p \leq 0.05$, ** $p \leq 0.01$, *** $p \leq 0.001$ relative to the FFD on Δ^8 -iso-THC).

3.2. Face centered designs: validation, coefficients and their significance

	$\Delta^{4(8)}$ -iso-THC		Δ^8 -iso-THC	
	<i>Experimental</i>	<i>Predicted</i>	<i>Experimental</i>	<i>Predicted</i>
<i>Value</i>	26.1	37.0	85.4	91.7
<i>Lower limit</i>	23.9	27.8	83.8	86.5
<i>Upper limit</i>	28.3	46.1	87.1	96.9

Table S3 Summary of the model validation for the face-centered designs; the independent validation experiments for $\Delta^{4(8)}$ -iso-THC and Δ^8 -iso-THC have been performed, respectively, at point $[-0.5, -0.6]$ and $[0.4, -0.5]$. For both models, experimental yield – calculated with pooled standard deviation from central replicates – fell within the model's predicted confidence interval (95% confidence level), confirming the validity of the proposed models.

FCD for the optimization of $\Delta^{4(8)}$ -iso-THC yield

<i>Coefficient</i>	<i>1 hour</i>		<i>2 hours</i>		<i>3 hours</i>	
	<i>Value</i>	<i>Significance</i>	<i>Value</i>	<i>Significance</i>	<i>Value</i>	<i>Significance</i>
b_0	26.1		18.0		12.6	
b_1	-8.1	***	-9.0	***	-7.8	***
b_2	-7.5	***	-3.4	*	-5.6	**
b_{12}	4.5	**	3.5	*	3.2	*
b_1^2	4.0	*	5.9	**	6.2	**
b_2^2	-0.1		-3.6	*	-0.7	

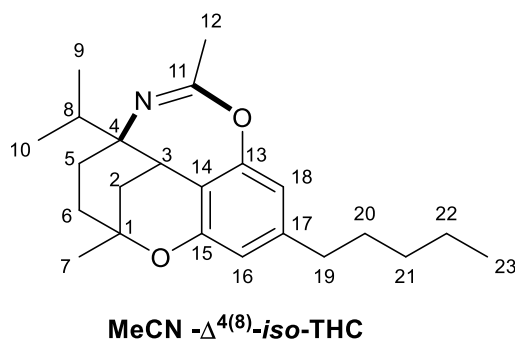
Table S4 Optimization of $\Delta^{4(8)}$ -iso-THC yield by FCD: coefficient values and their significance (* $p \leq 0.05$, ** $p \leq 0.01$, *** $p \leq 0.001$).

FCD for the optimization of Δ^8 -iso-THC yield

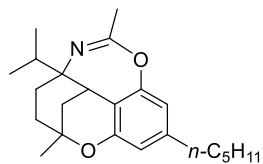
<i>Coefficient</i>	<i>1 hour</i>		<i>2 hours</i>		<i>3 hours</i>	
	<i>Value</i>	<i>Significance</i>	<i>Value</i>	<i>Significance</i>	<i>Value</i>	<i>Significance</i>
b_0	90.7		85.7		80.4	
b_1	0.2		-5.8	***	-9.3	***
b_2	-5.2	***	-18.7	***	-17.9	***
b_{12}	-11.9	***	-11.5	***	-13.5	***
b_1^2	-9.3	***	-6.5	**	-5.6	**
b_2^2	-10.6	***	-12.8	***	-10.6	***

Table S5 Optimization of Δ^8 -iso-THC yield by FCD: coefficient values and their significance (* $p \leq 0.05$, ** $p \leq 0.01$, *** $p \leq 0.001$).

4. ^1H and ^{13}C NMR Spectra for the isolated compounds

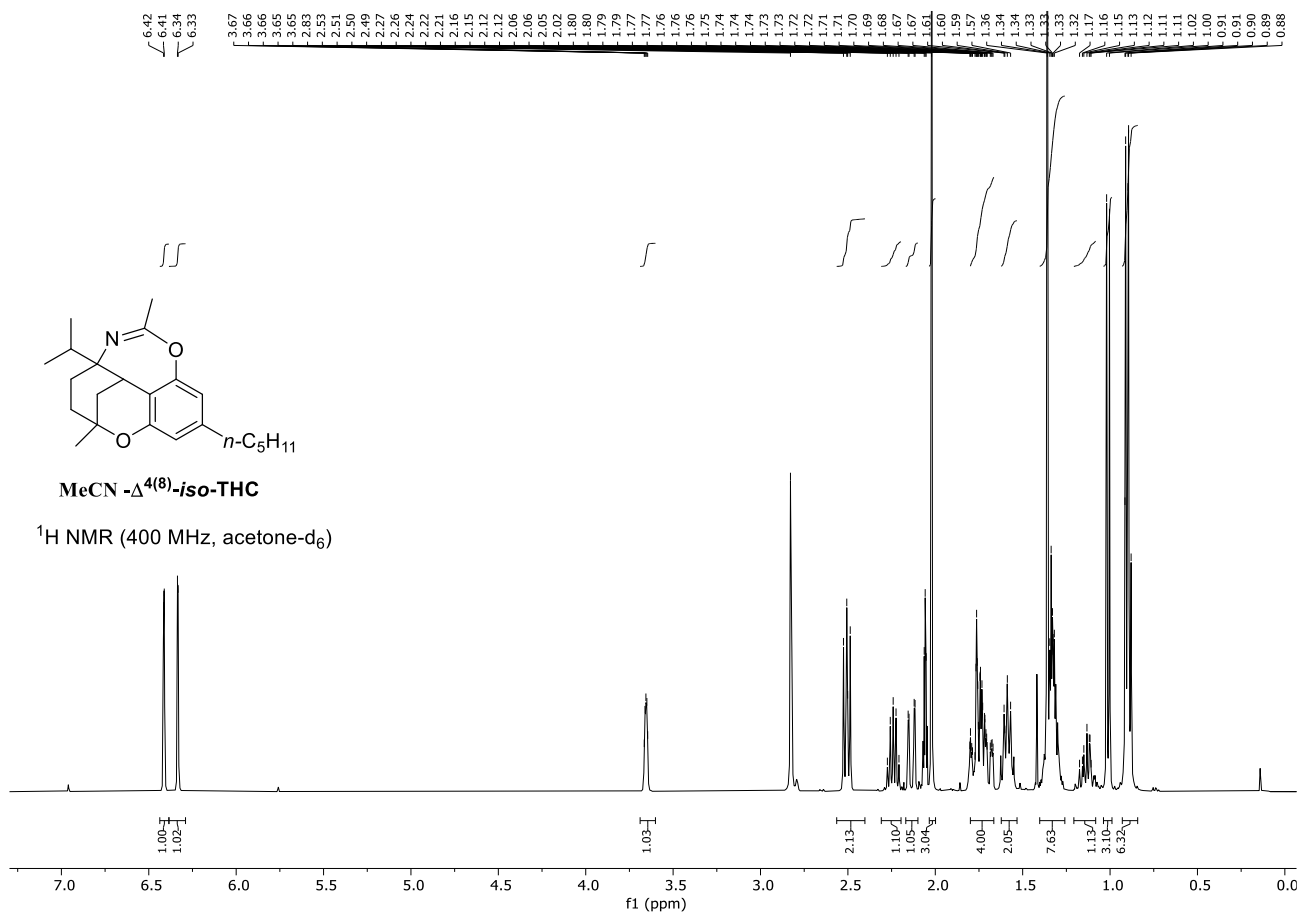


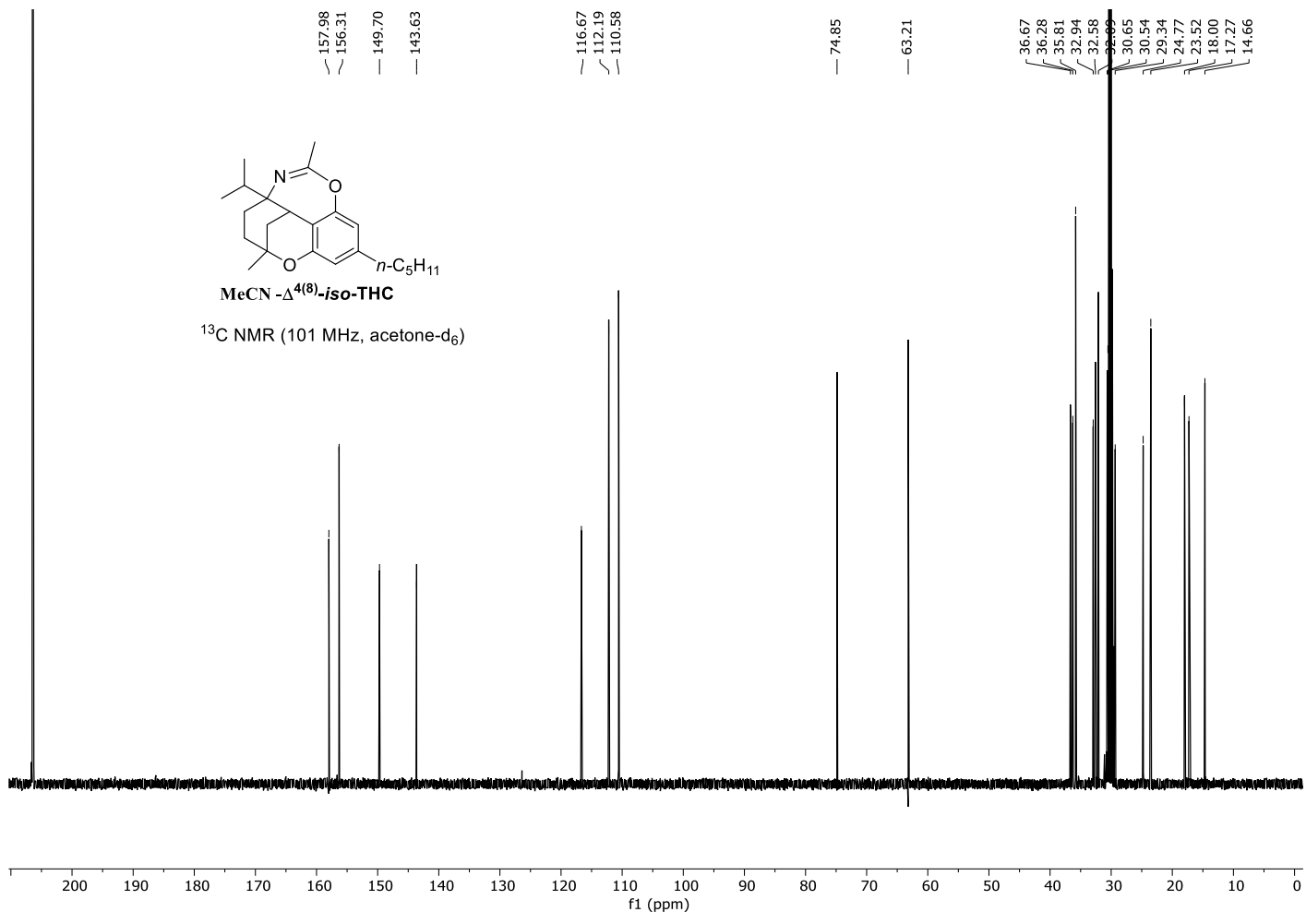
MeCN- $\Delta^{4(8)}$ -iso-THC. ^1H NMR (400 MHz, CD_3COCD_3) δ 6.41 (d, $J = 1.5$ Hz, 1H), 6.33 (d, $J = 1.5$ Hz, 1H), 3.66 (dt, $J = 4.1, 1.7$ Hz, 1H, H-3), 2.56 – 2.40 (m, 2H, H-19), 2.24 (p, $J = 6.7$ Hz, 1H, H-8), 2.14 (dd, $J = 13.8, 2.0$ Hz, 1H, H-2), 2.02 (s, 3H, H-12), 1.83 – 1.65 (m, 4H, H-5, H-6, H-2), 1.59 (p, $J = 7.5$ Hz, 2H, H-20), 1.40 – 1.26 (m, 7H, H-7, H-21, H-22), 1.19 – 1.08 (m, 1H, H-5), 1.01 (d, $J = 6.5$ Hz, 3H, H-10), 0.90 (m, 6H, H-9 and H-23). ^{13}C NMR (101 MHz, CD_3COCD_3) δ 158.0, 156.3, 149.7 (C-11), 143.6, 116.7, 112.2 (CH), 110.6 (CH), 74.8 (C-1), 63.2 (C-4), 36.7 (CH_2 , C-19), 36.3 (CH_2 , C-6), 35.8 (CH, C-3), 32.9 (CH_2 , C-2), 32.6 (CH_2 , C-21), 32.1 (CH_2 , C-20), 30.7 (CH_2 , C-5), 30.5 (CH, C-8), 29.3 (CH_2 , C-22), 24.8 (CH_3 , C-12), 23.5 (CH_3 , C-7), 18.0 (CH_3 , C-10), 17.3 (CH_3 , C-9), 14.7 (CH_3 , C-23).



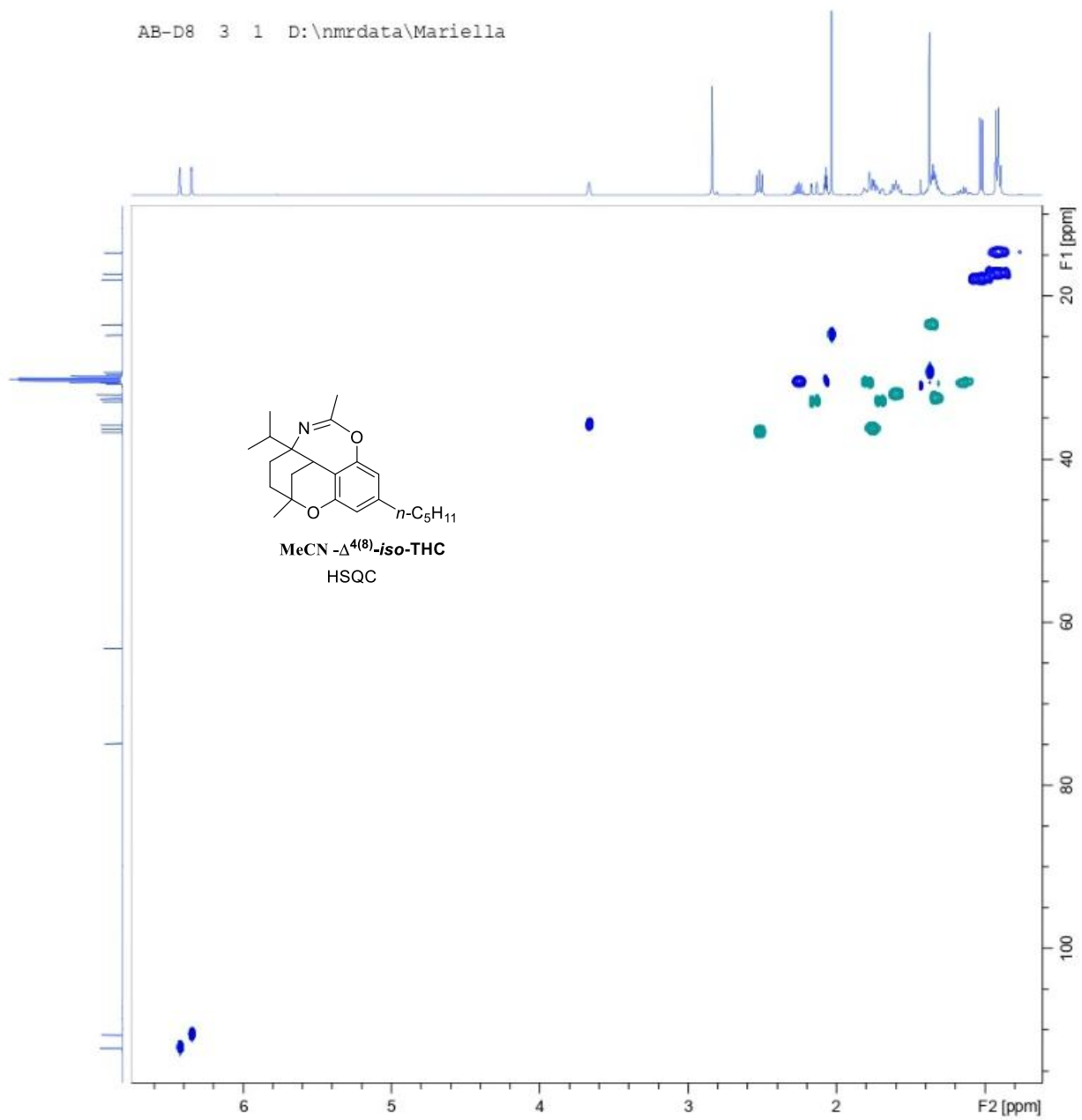
MeCN- $\Delta^4(8)$ -iso-THC

^1H NMR (400 MHz, acetone- d_6)

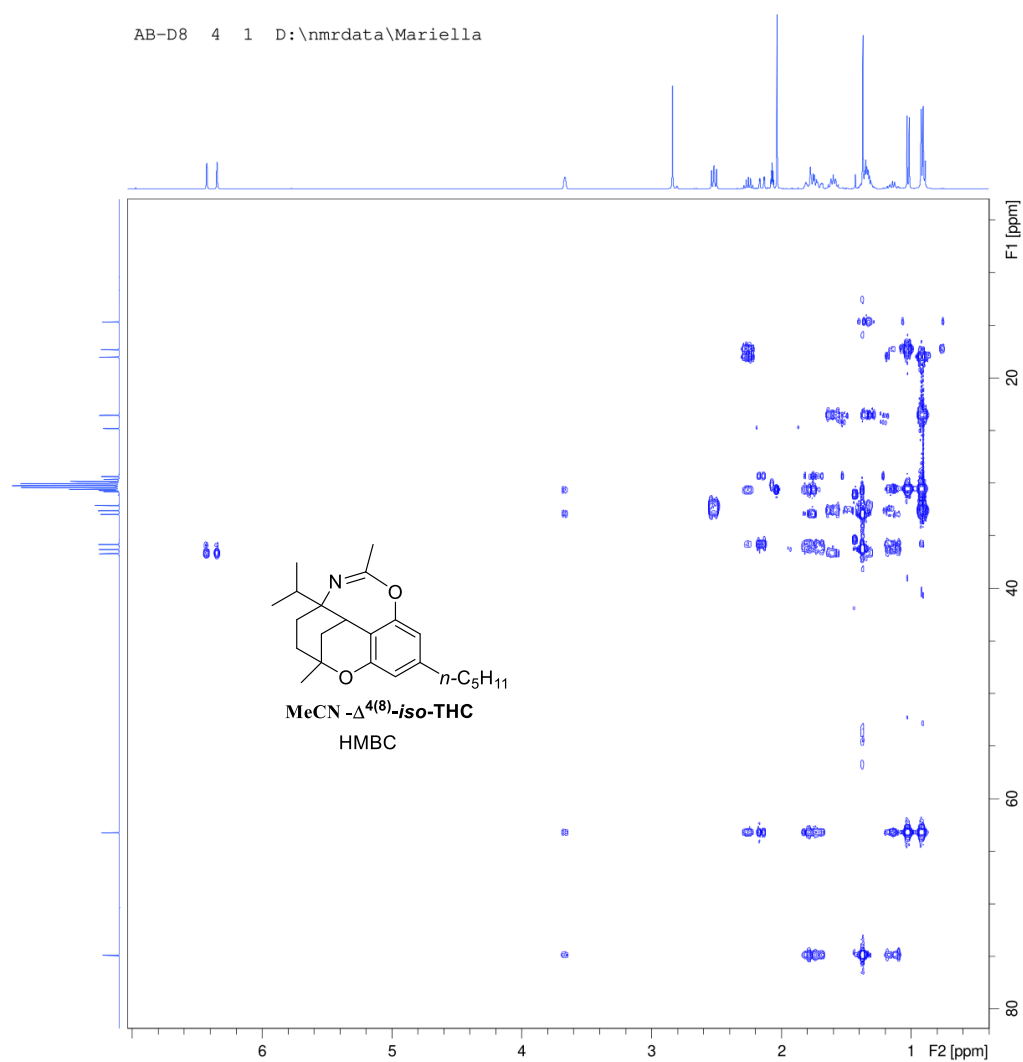




Heteronuclear single quantum coherence (HSQC) spectra for compound MeCN- $\Delta^{4(8)}$ -*iso*-THC (Acetone- d_6)

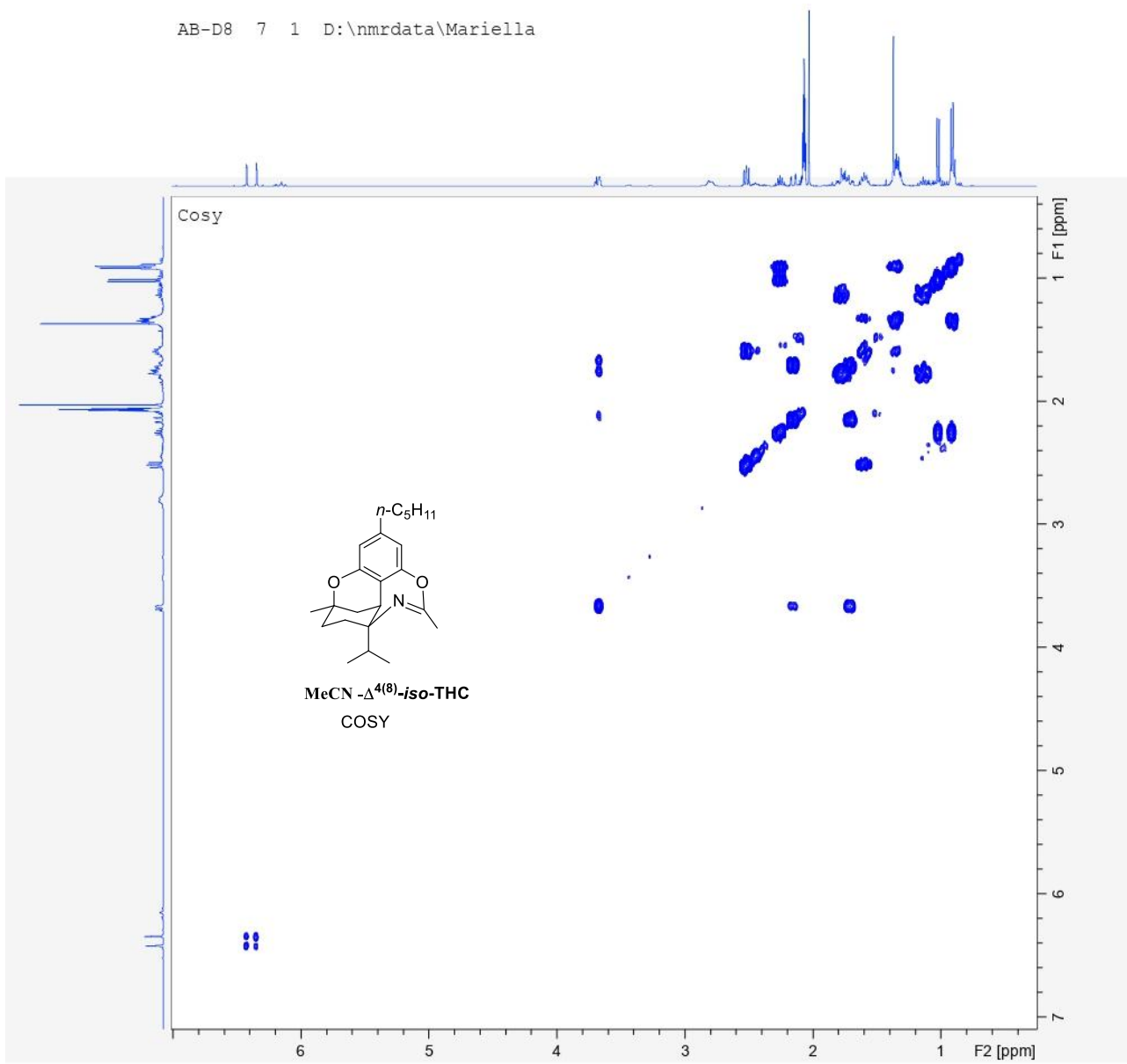


Heteronuclear Multiple Bond Correlation (HMBC) spectra for compound MeCN- $\Delta^{4(8)}$ -*iso*-THC (Acetone- d_6)

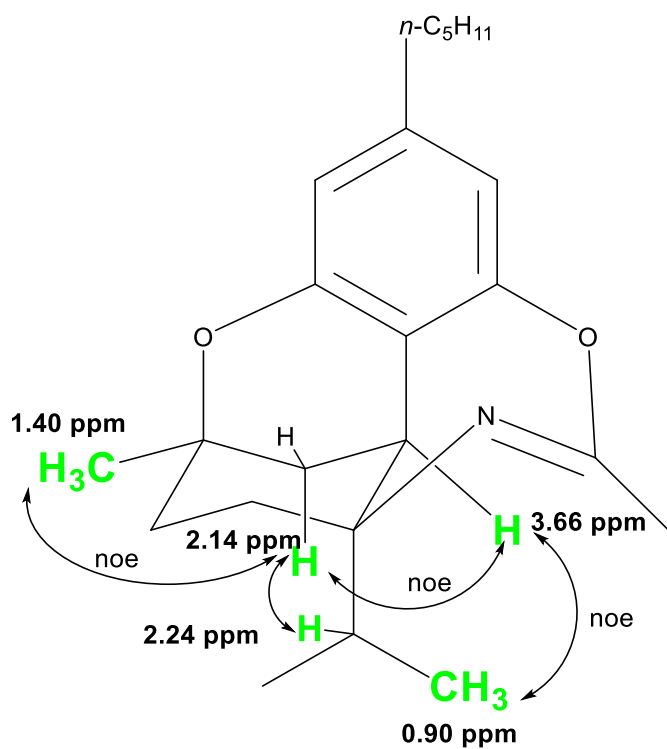


Correlation Spectroscopy analysis (COSY) for compound MeCN- $\Delta^{4(8)}$ -iso-THC (Acetone- d_6)

AB-D8 7 1 D:\nmrdata\Mariella

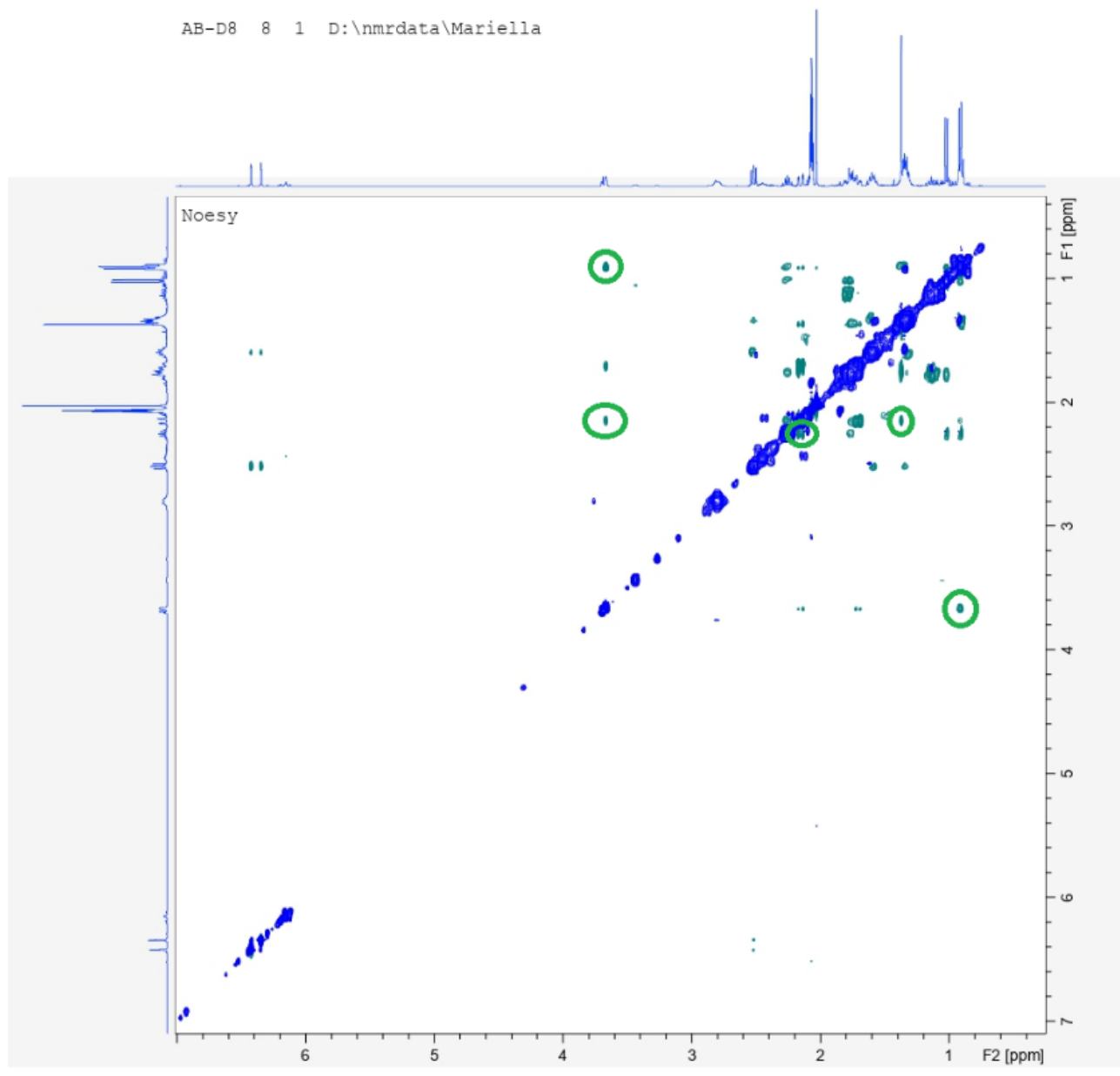


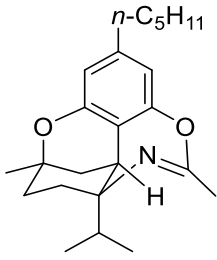
Nuclear Overhauser Effect Spectrum (NOESY) for compound MeCN- $\Delta^{4(8)}$ -iso-THC (Acetone- d_6)



Nuclear Overhauser Effect Spectrum (NOESY) for compound MeCN- $\Delta^{4(8)}$ -iso-THC (Acetone- d_6)

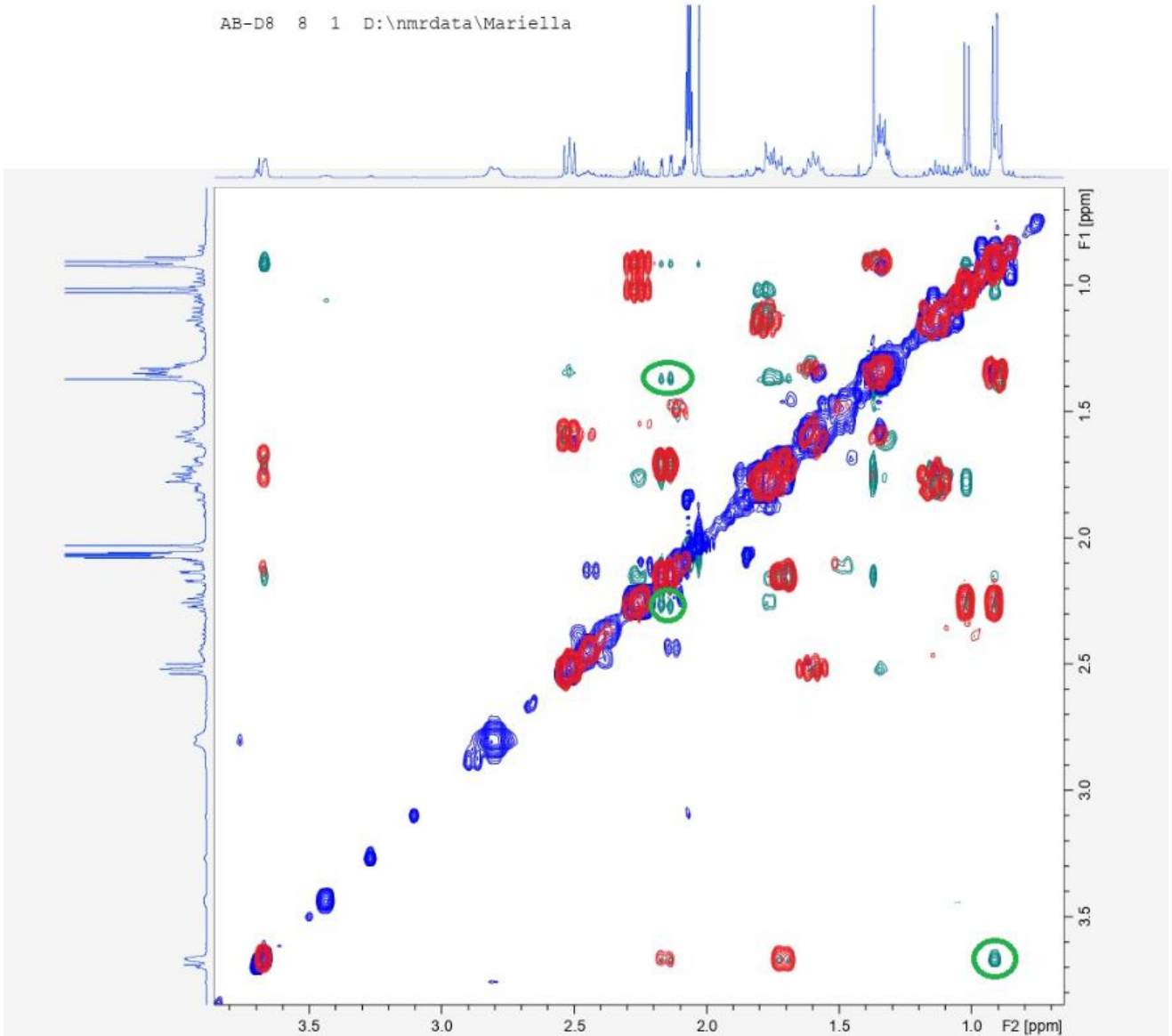
AB-D8 8 1 D:\nmrdata\Mariella

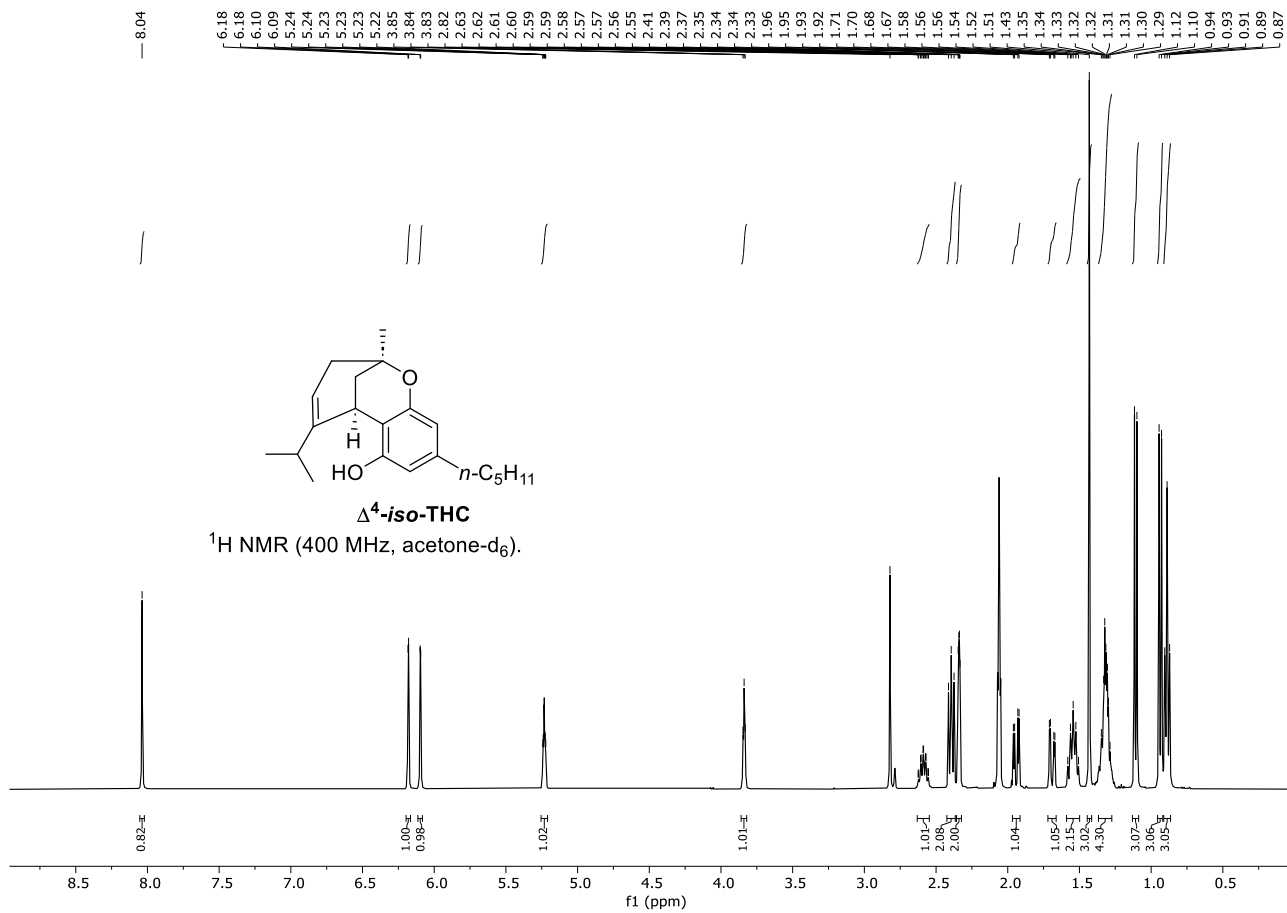




MeCN - $\Delta^{4(8)}$ -iso-THC
NOESY + COSY

AB-D8 8 1 D:\nmrdata\Mariella





155.47
153.30
149.31

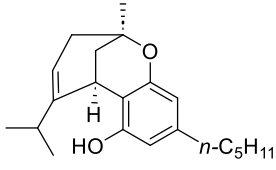
141.22

114.40
111.58
107.65
105.91

73.36

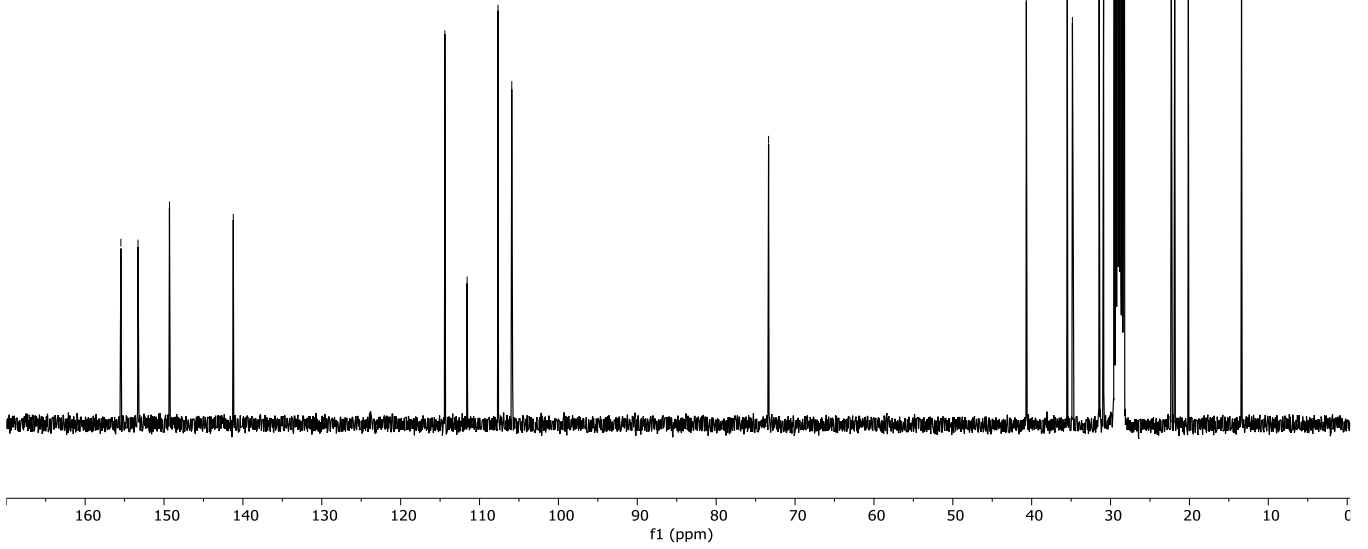
40.68
35.49
34.83
31.45
31.39
30.88

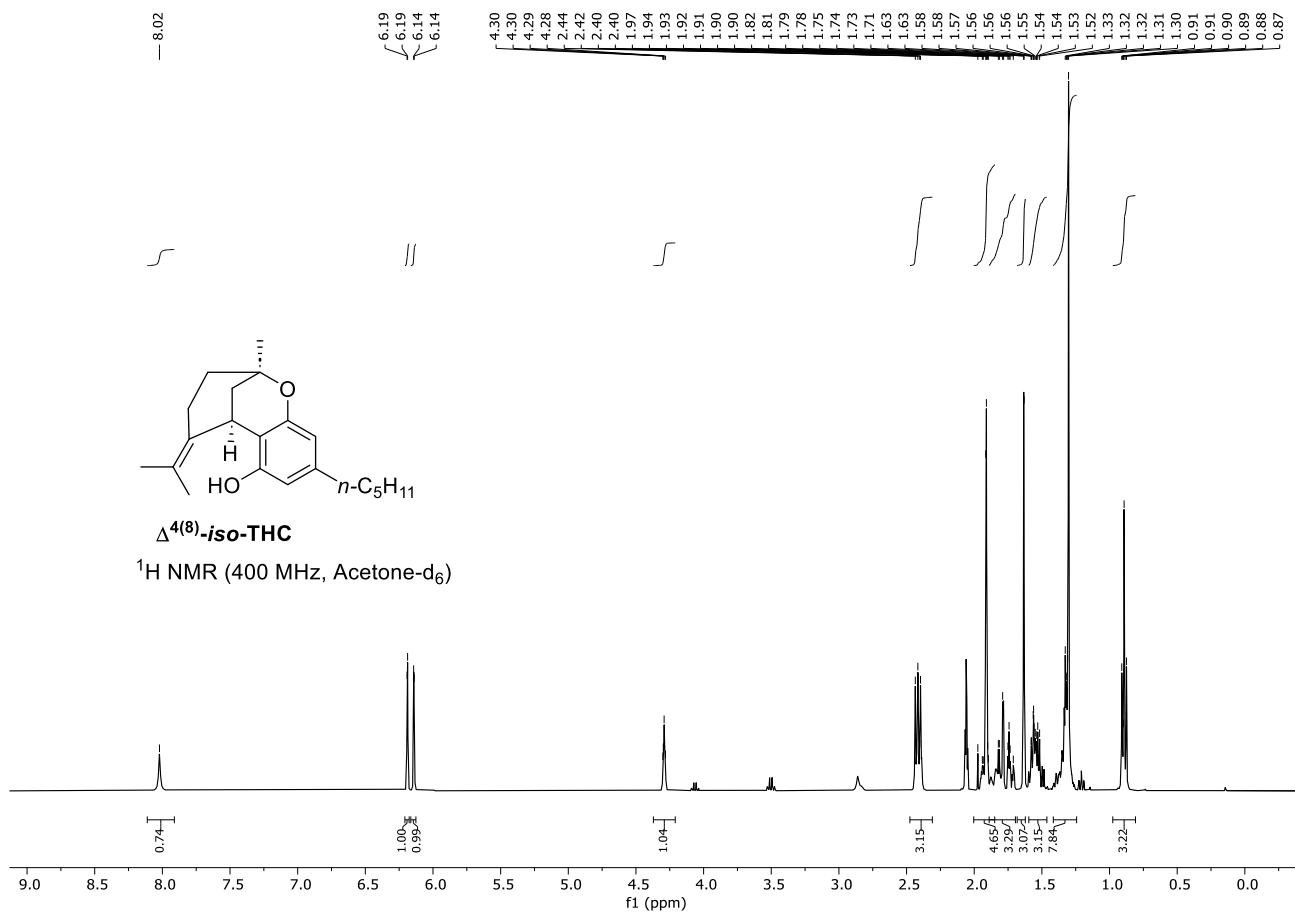
28.41
22.30
21.87
20.13
13.40

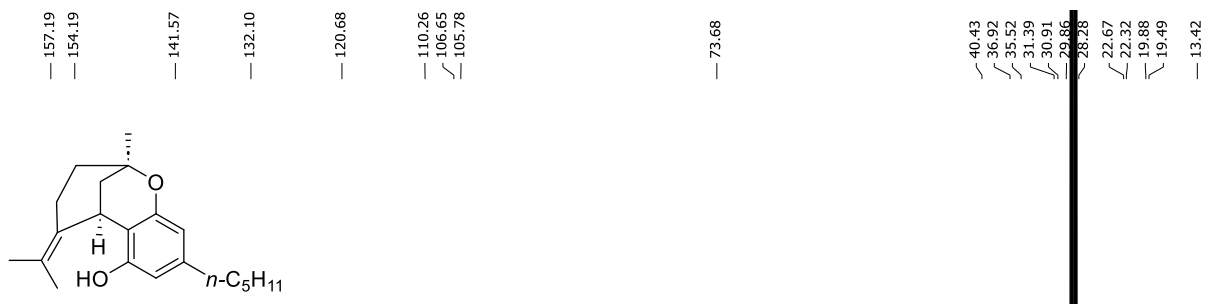


Δ^4 -*iso*-THC

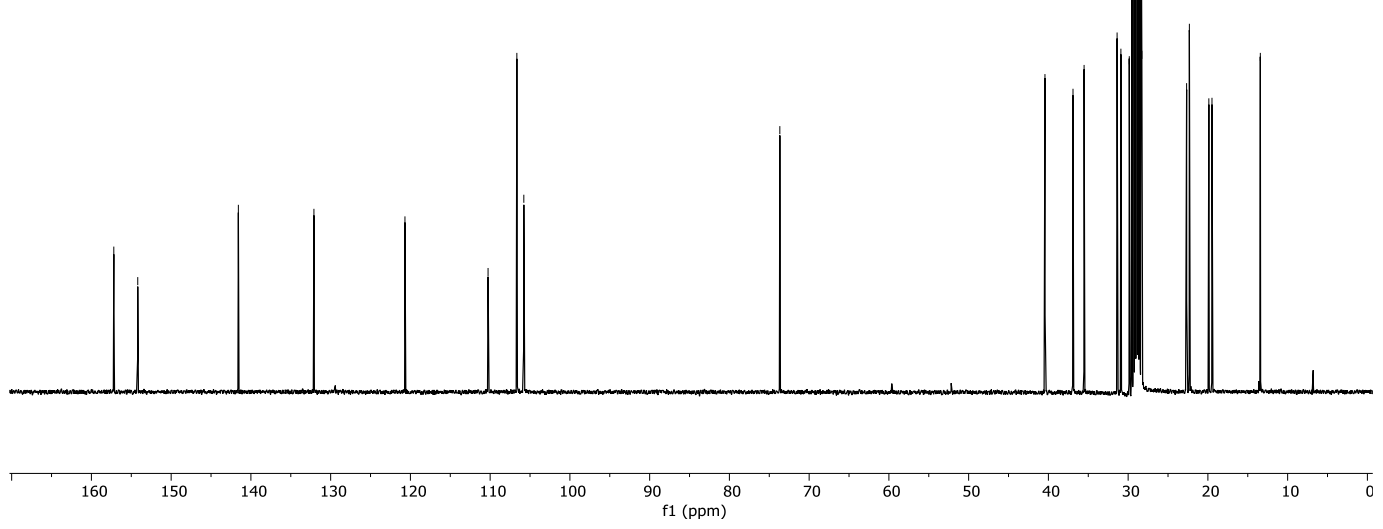
¹³C NMR (101 MHz, acetone-d₆).

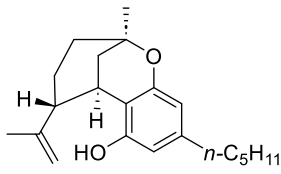






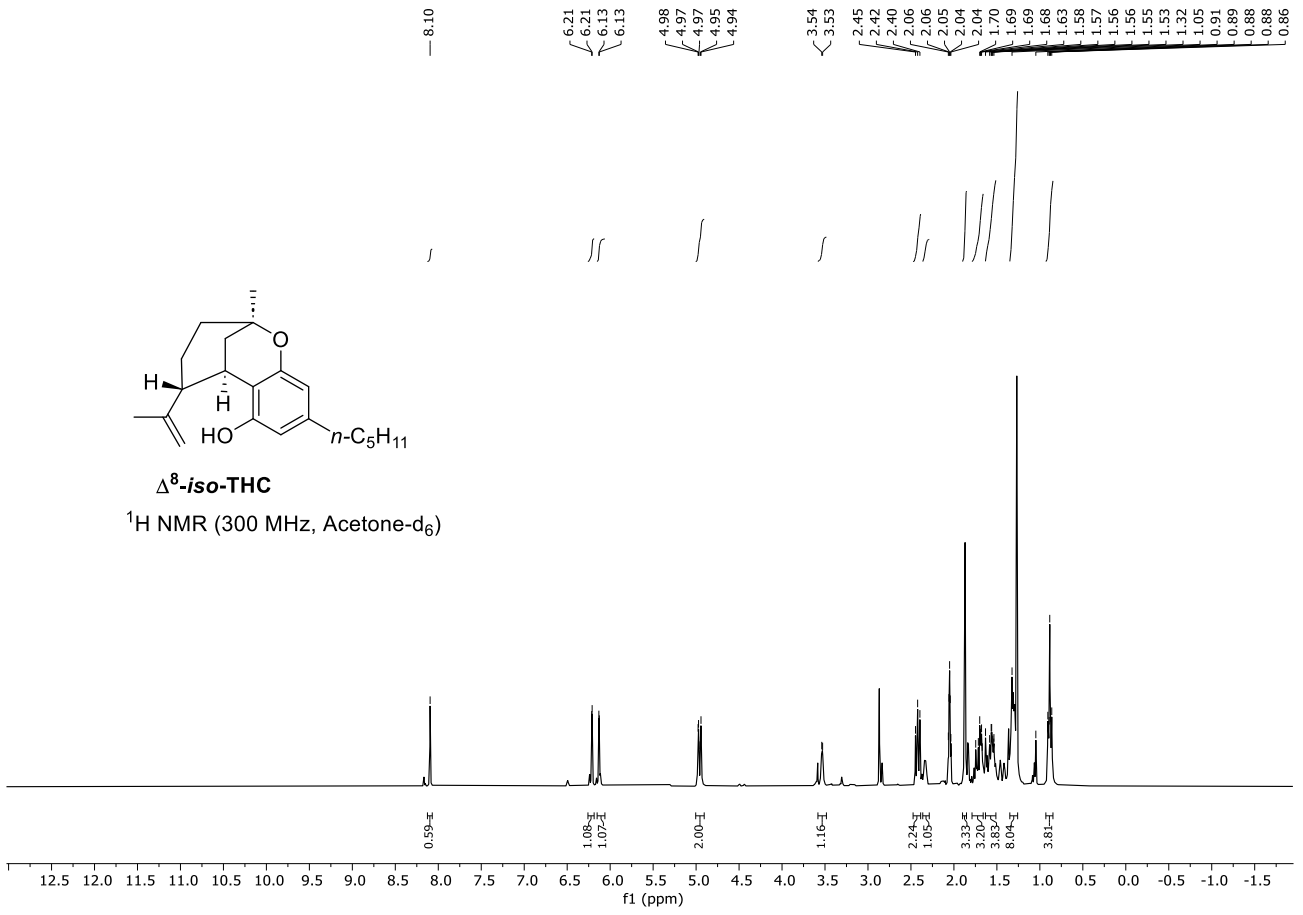
$\Delta^{4(8)}$ -iso-THC
 ^{13}C NMR (101 MHz, Acetone- d_6)

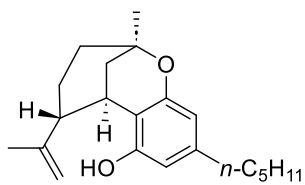




Δ^8 -*iso*-THC

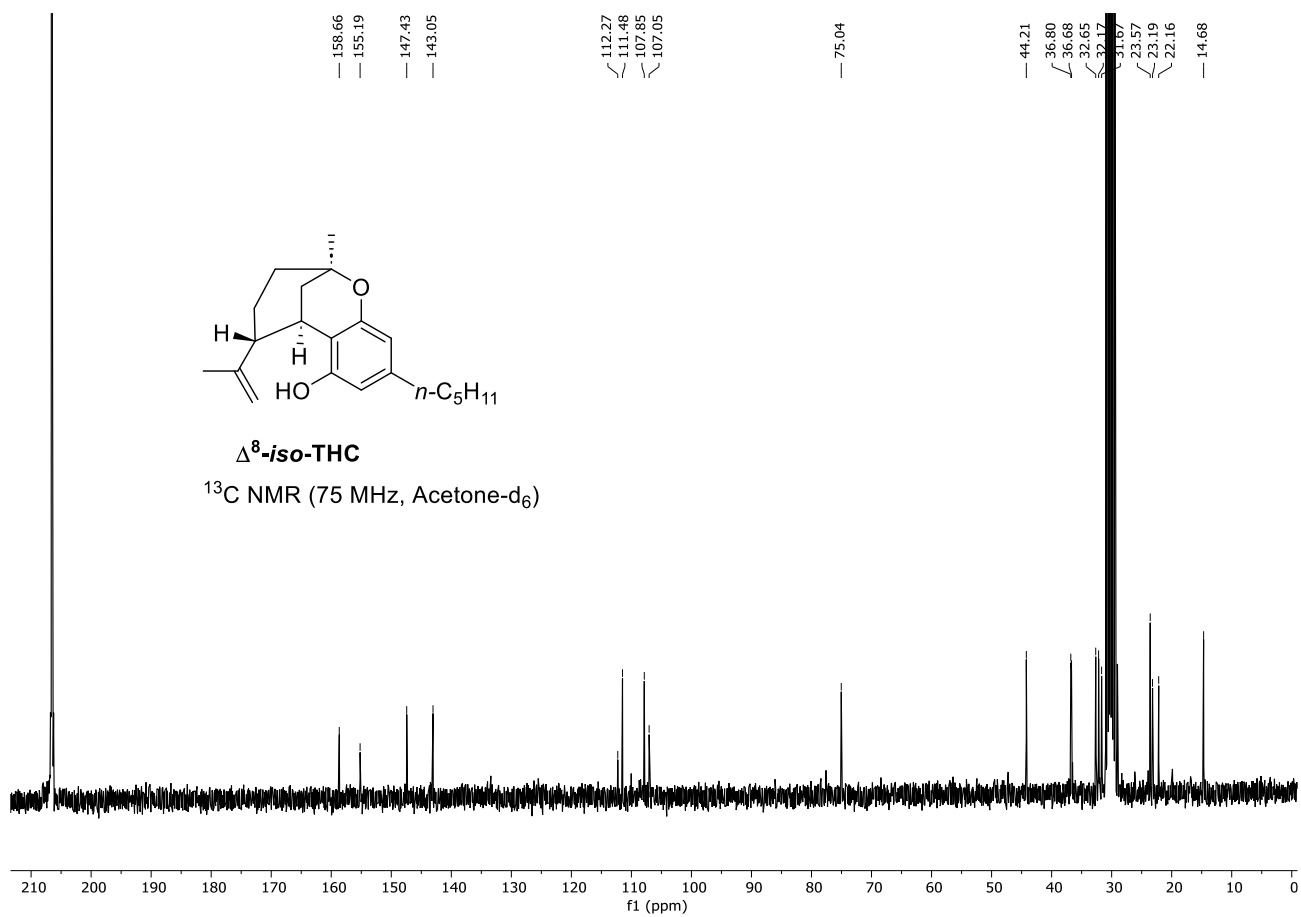
^1H NMR (300 MHz, Acetone- d_6)

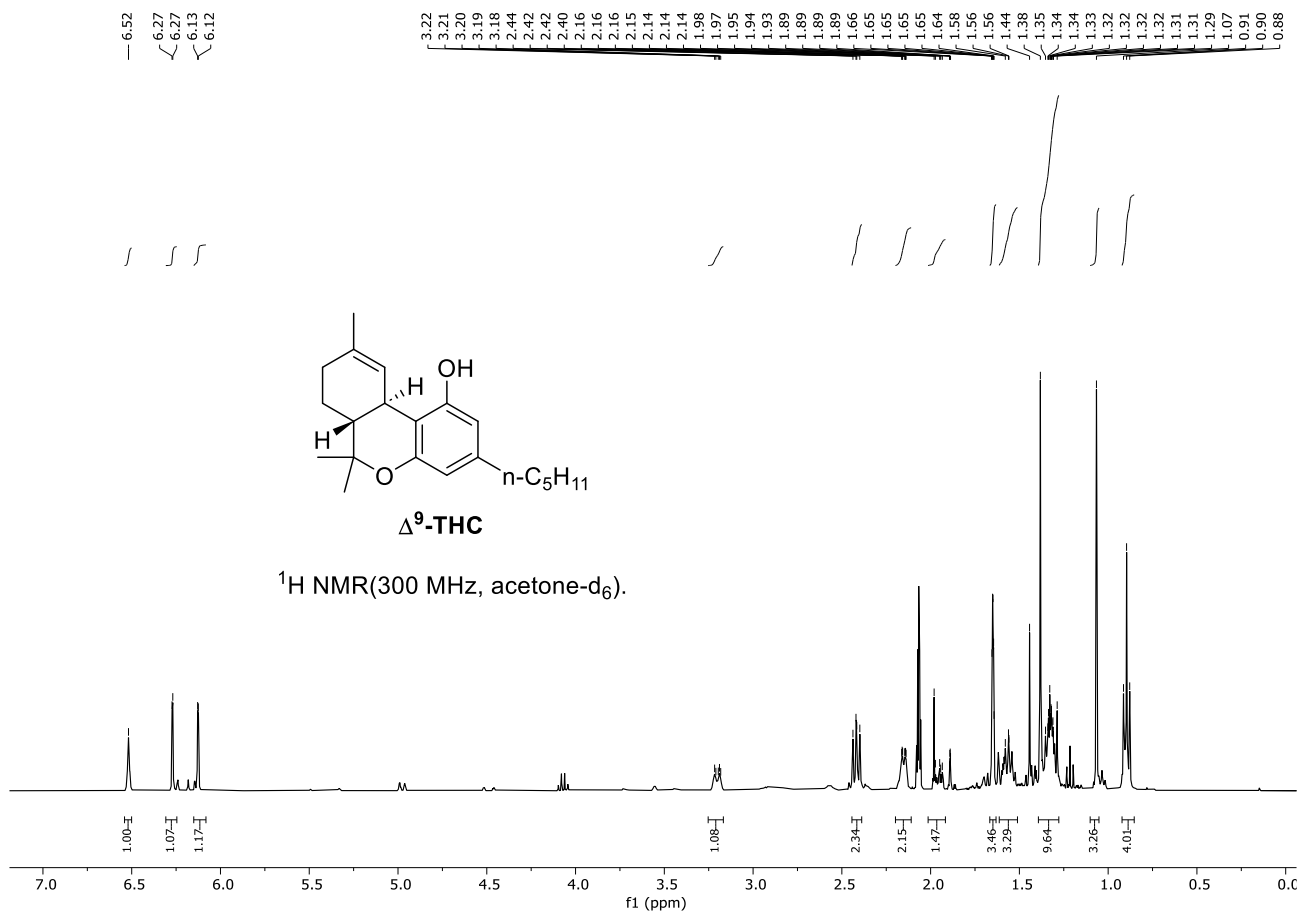




Δ^8 -iso-THC

^{13}C NMR (75 MHz, Acetone- d_6)





157.26
156.10

143.19

133.38

126.29

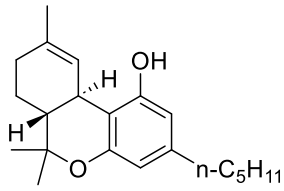
110.23
110.01
108.53

77.58

47.28

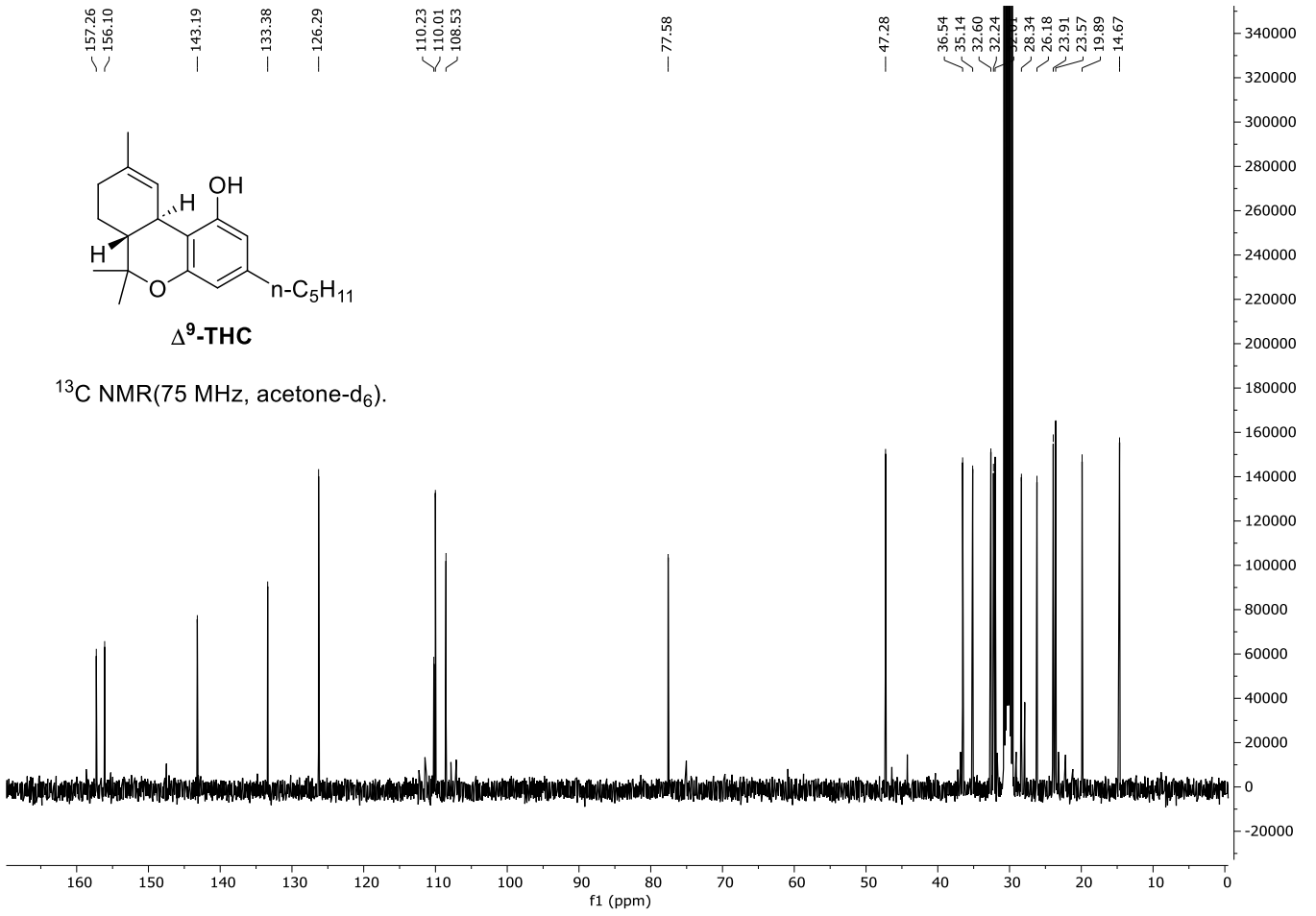
36.54
35.14
32.60
32.24

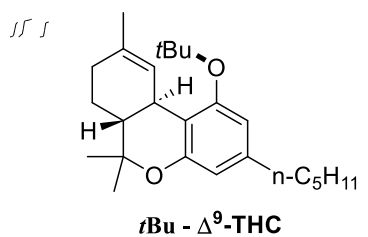
28.91
28.34
26.18
23.91
23.57
19.89
14.67



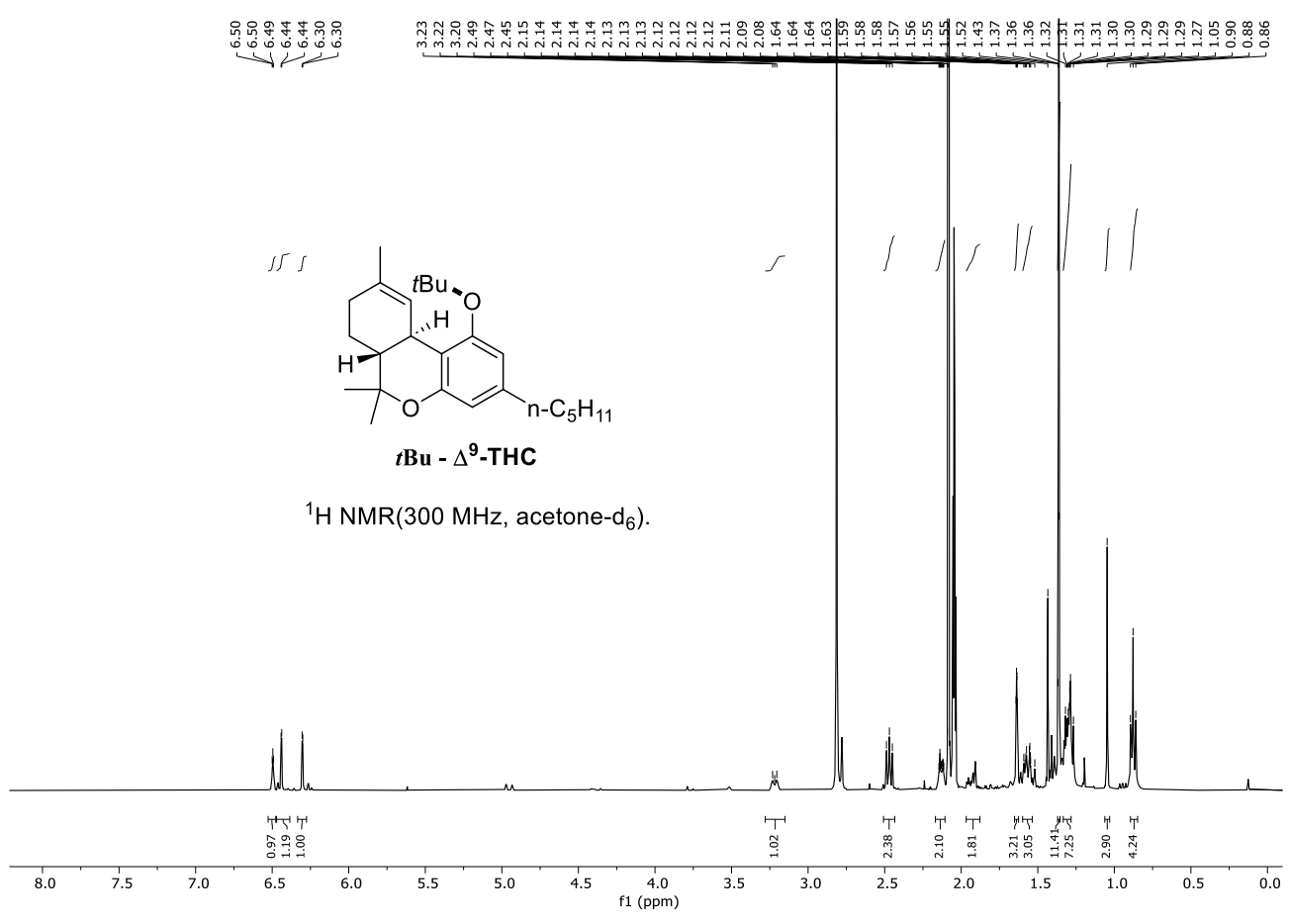
Δ^9 -THC

^{13}C NMR(75 MHz, acetone- d_6).

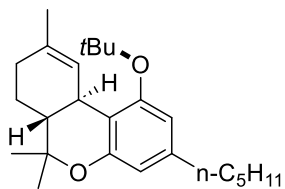




¹H NMR(300 MHz, acetone-d₆).

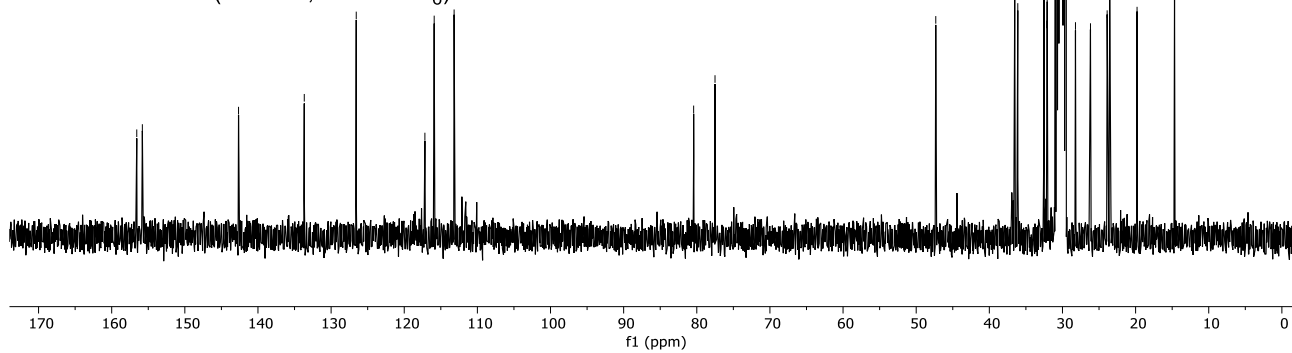


\sim 156.57
 \sim 155.81
 — 142.66
 — 133.67
 — 126.56
 \sim 117.18
 \sim 115.91
 \sim 113.18
 — 80.43
 — 77.51
 — 47.32
 \sim 36.53
 \sim 36.11
 \sim 32.53
 \sim 32.15
 \sim 28.22
 \sim 26.17
 \sim 23.89
 \sim 23.54
 \sim 19.80
 — 14.68



tBu - Δ^9 -THC

^{13}C NMR (75 MHz, acetone- d_6).



5. Exact mass results

MeCN - $\Delta^{4(8)}$ -*iso-THC*, HRMS m/z : $[M+H]^+$ calcd for $C_{23}H_{33}O_2N$ 356.2584; found 356.2581.

Found elemental compositions								
Hit	Formula	m/z	RDB	ppm	MS Rank	MSMS ppm	MSMS Rank	Found
1	C ₂₃ H ₃₃ NO ₂	356.2584	8.0	-0.9	1			NA/NA

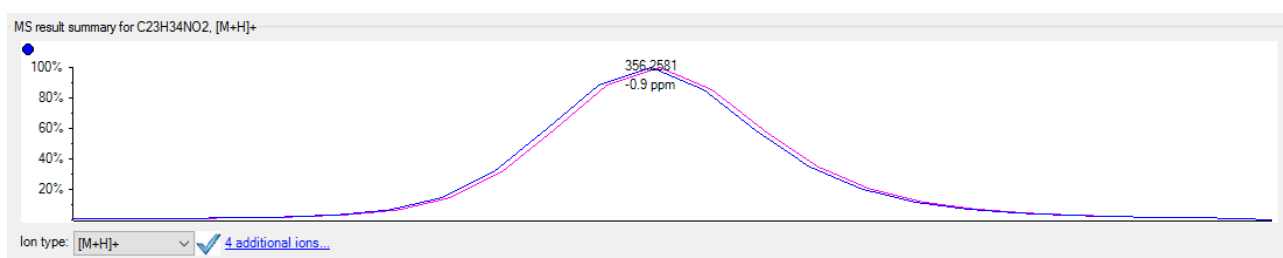


Fig. S35 HRMS peak obtained from the analysis of isolated *MeCN* - $\Delta^{4(8)}$ -*iso-THC*.

Δ^4 -iso-THC, HRMS m/z : $[M+H]^+$ calcd for $C_{21}H_{30}O_2$ 315.2319, found 315.2310

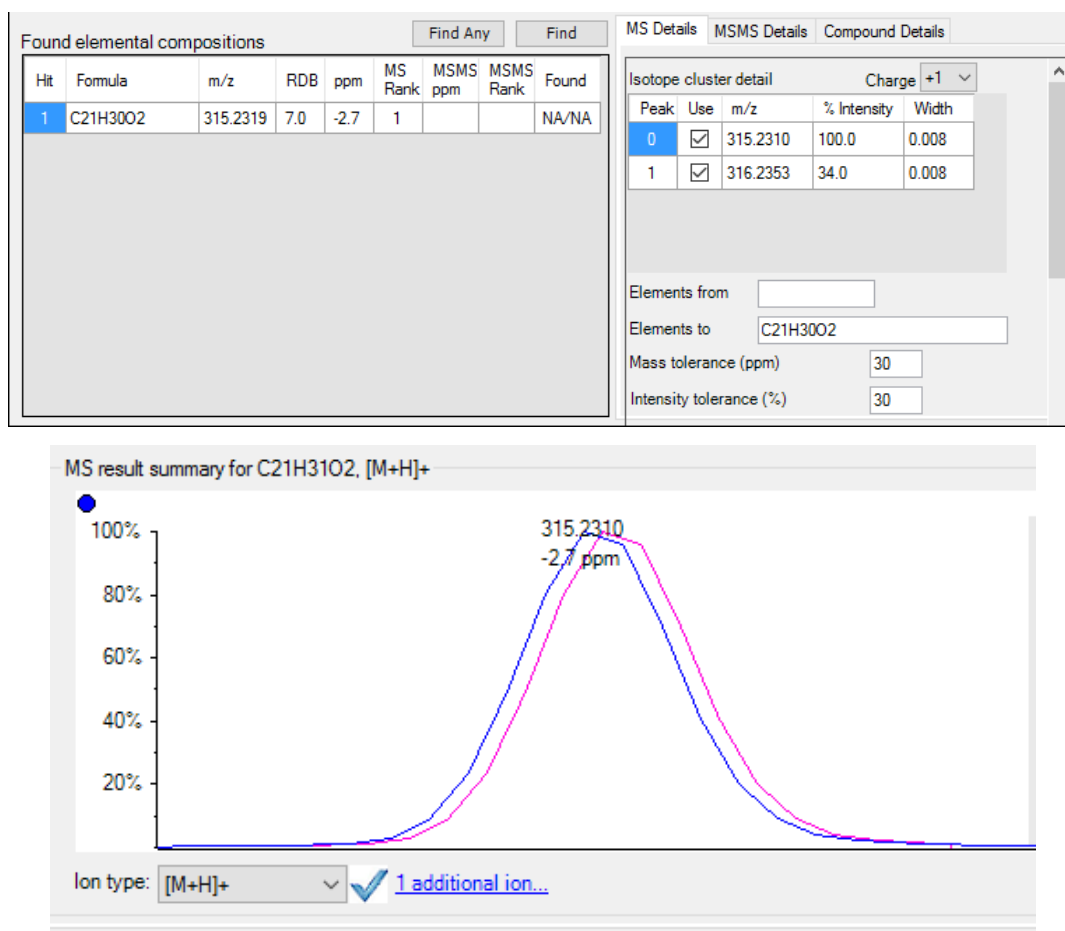


Fig. S36 HRMS peak obtained from the analysis of isolated Δ^4 -iso-THC.

$\Delta^{4(8)}$ -*iso*-THC, HRMS m/z : $[M+H]^+$ calcd for $C_{21}H_{30}O_2$ 315.2319; found 315.2316

Found elemental compositions									MS Details				
Hit	Formula	m/z	RDB	ppm	MS Rank	MSMS ppm	MSMS Rank	Found	Isotope cluster detail	Charge			
1	C ₂₁ H ₃₀ O ₂	315.2319	7.0	-0.8	1			NA/NA	Peak	Use	m/z	% Intensity	Width
									0	<input checked="" type="checkbox"/>	315.2316	100.0	0.008
									1	<input checked="" type="checkbox"/>	316.2355	25.9	0.009

Elements from:
Elements to: C₂₁H₃₀O₂
Mass tolerance (ppm): 30
Intensity tolerance (%): 30
#C/#heteroatoms greater than: 0

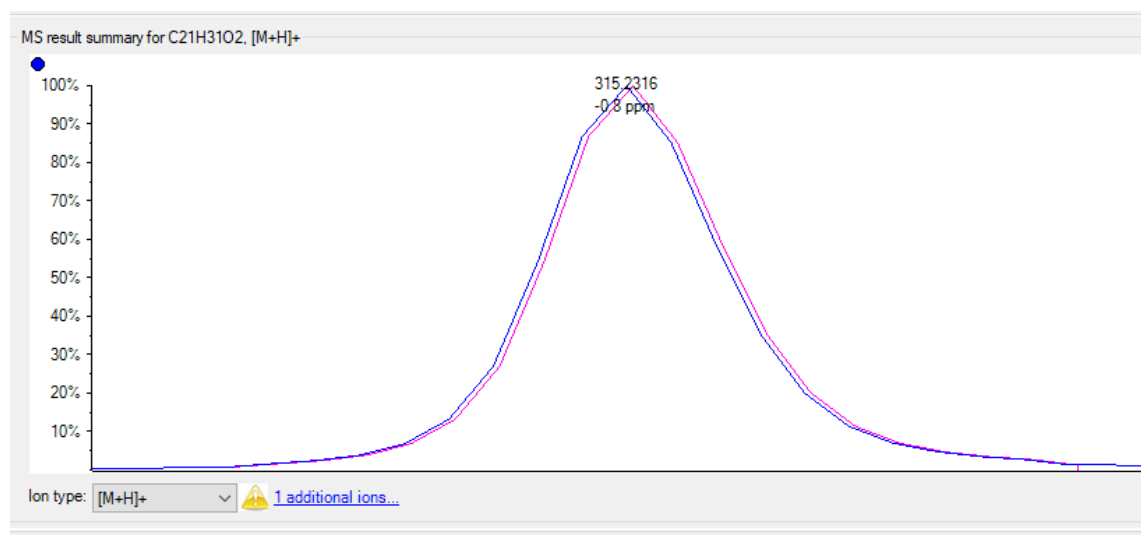


Fig. S37 HRMS peak obtained from the analysis of isolated $\Delta^{4(8)}$ -*iso*-THC.

1-(tert-butoxy)-6,6,9-trimethyl-3-pentyl-6a,7,8,10a-tetrahydro-6H-benzo[c]chromene (*tBu- $\Delta^4(8)$ -iso-THC*), HRMS m/z : $[M+H]^+$ calcd for $C_{25}H_{39}O_2$ 371.2945, found 371.2940

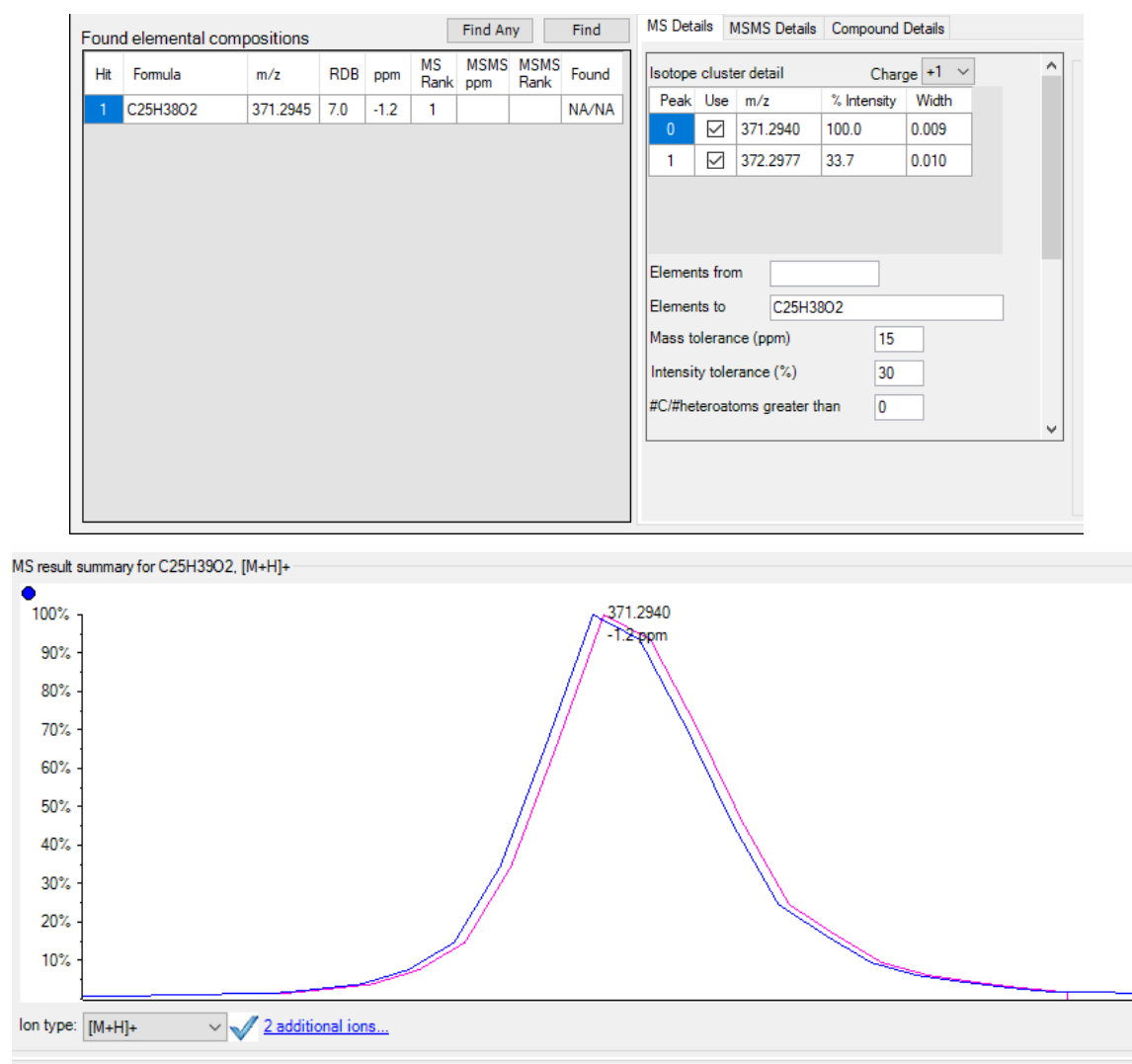


Fig. S38 HRMS peak obtained from the analysis of isolated *tBu- $\Delta^4(8)$ -iso-THC*.